Journal of Materials Chemistry A

REVIEW

View Article Online
View Journal | View Issue

Cite this: J. Mater. Chem. A, 2019, 7, 21004

The synthetic strategies of metal–organic framework membranes, films and 2D MOFs and their applications in devices

Haolin Zhu and Dingxin Liu *

Metal–organic frameworks (MOFs) are now attracting more and more attention due to their various special properties and functions. They are regarded as potential candidates for gas separation, adsorption, chemical sensing, catalysis and many other applications. Many types of two-dimensional (2D) architectures are developed, which exhibit great potential in charge transfer, catalysis, luminescence and so on. 2D architectures based on MOFs are developed, including MOF membranes, MOF thin films and 2D MOFs. Herein, we mainly overview the synthetic methods and device applications of these MOF-based 2D architectures, and finally proposed some prospects for the development of these MOF materials. Some key scientific problems and their possible solutions are also proposed in this review.

Received 21st May 2019
Accepted 27th August 2019

DOI: 10.1039/c9ta05383b

rsc.li/materials-a

1. Introduction

Since the definition of metal–organic frameworks (MOFs) in 1995 by Yaghi *et al.*,[1] MOFs have attracted much attention from many researchers due to their potential in separation, adsorption, catalysis, chemical sensors, miniaturized electronic equipment, optical materials, drug delivery, NLO materials, electronic and optoelectronic devices and so on.[2–13] Their structure tailorability, vast diversity,[14–18] high thermal as well as mechanical stability and organic functionality[19–21] have attracted much attention. Supramolecular building blocks[22] and secondary building units (SBUs)[23] can be used to design the structure of MOFs at the level of building units rather than the level of primary building blocks.[2]

Recently, two-dimensional (2D) architecture materials, such as graphene,[24,25] metal nanosheets,[26] and 2D hexagonal boron nitride,[27,28] have exhibited great potential in electrochemistry,[24] light-emission,[29] gas separation[30] and so on. Since Furukawa *et al.* divided hierarchically structured MOF architectures into four categories,[31] those MOFs with 2D architectures such as MOF thin films, membranes and 2D MOFs have received more and more attention. The thickness of 2D MOFs is mainly on the atomic scale, and the thickness of MOF thin films can range

State Key Laboratory of Optoelectronic Materials and Technologies, Nanotechnology Research Center, School of Materials Science & Engineering, Sun Yat-sen University, Guangzhou 510275, Guangdong, China. E-mail: liudx9@mail.sysu.edu.cn

Haolin Zhu was born in 1998, Shandong Province, China. He is studying at the School of Materials Science and Engineering, Sun Yat-Sen University in Guangzhou, China. He is now doing his research under the supervision of Prof. Dr Dingxin Liu.

Prof. Dr Dingxin Liu received his Ph.D from Shanghai Jiao Tong University. After graduation he worked as an assistant Professor at the National Center for Nanoscience and Technology, Chinese Academy of Sciences, Beijing, P. R. China. In 2017 he began his career as an associate Professor at the School of Materials Science and Engineering, Sun Yat-sen University, Guangzhou, China. His current research focuses on Metal–Organic Frameworks (MOFs), Porous Coordination Polymers (PCPs), Nanomaterials, Materials for Energy and Environment, Photoelectric Functional Materials and so on.

from the nanoscale to the millimeter scale, while MOF membranes mainly represent the membranes with adsorption, separation or separation-based functions (Fig. 1). 2D MOFs could be exfoliated from MOF thin films which are composed of MOF nanolayers. MOF membranes should have adsorption, separation or separation-based functions (*i.e.* battery systems, which will be discussed later), but MOF films do not have this restriction. That is, the differences between MOF membranes and thin films mostly lie in the functions, rather than in chemical essence. Various properties of MOF membranes, thin films and 2D MOFs have been developed, and efforts towards the improvement of these materials are being carried out.

Generally speaking, in order to optimize the properties of MOFs, we can start from choosing a suitable synthetic strategy, metal ions and organic ligands,[32] chemically modifying using various functional groups, designing MOFs with a variety of different topologies[33] and combining MOFs with other materials to obtain various composites.[34,35] The metal ion clusters of most MOFs are based on di- or trivalent ions of 3p and 3d metals or lanthanides.[36] And especially, many kinds of MOF membranes, films and 2D MOFs are based on d^{10} metal ions. The d^{10} metal configuration is related to the coordination environment, so they are very suitable for the construction of coordination polymers, the structure of which can be finely tuned.[37,38] Each gram of MOF material has a surface area of up to several thousand square meters. The pore size can be adjusted by selecting an appropriate linker, the metal ion centre, and controlling the reaction conditions.[39] The physicochemical properties and topological structure of MOFs mainly depend on the binding sites and the orientation of their organic ligands, and the coordination number and geometry of metal ion clusters.[40] In view of the above aspects, MOFs with improved properties and various functionalities could be designed and prepared, and MOF membranes, films and 2D MOFs could be further improved.

Since some excellent reviews have summarized MOF membranes, thin films, 2D MOFs and their device applications[41] respectively, here we review the synthetic methods of MOF membranes, thin films and 2D MOFs, and some applications, including some latest research. Some strategies to improve the properties of these MOF materials are also summarized. Finally, the prospects for their development have also been proposed.

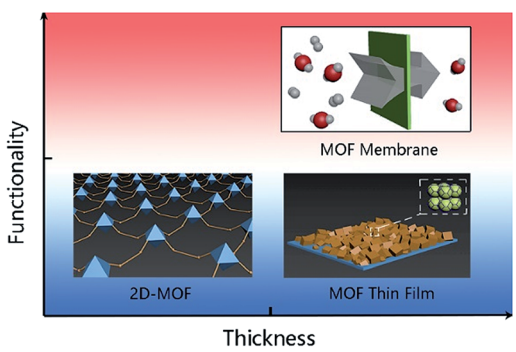

Fig. 1 The difference between MOF thin films, MOF membranes and 2D MOFs.

2. 2D MOFs

Two-dimensional materials have attracted much attention since graphene was discovered in 2004.[42] As a new class of 2D materials, 2D MOFs have been marked by their high conductivity, chemical tunability and high structural porosity,[43,44] and usually exhibit three, four or six connected network topologies.[45] Generally, three available metal coordination sites are usually contained in the metal complexes of the MOF to construct the 2D structure.[46,47] 2D polymers have become research hotspots, including graphene and 2D MOFs.[48] The synthetic methods of different 2D MOFs are various, including the Langmuir–Blodgett method, sonication exfoliation, mechanical exfoliation and the like. Besides, many aspects of 2D MOFs have already been studied, including chirality,[49] magnetism,[50] and luminescence.[51] In general, several kinds of methods have been used to prepare 2D MOFs. Although excellent reviews about 2D MOFs have been published recently,[30,52] here we mainly introduce some novel synthetic strategies together with classical method, and some special properties and characterization of 2D MOFs are also mentioned.

2.1 Synthetic methods of 2D MOFs

Similar to most nanomaterials, according to the synthetic approaches of 2D MOFs, the synthetic methods could be generally divided into bottom-up and top-down strategies.[30] Briefly, the bottom-up strategy refers to the direct assembly of metal ions and organic ligands to construct the MOF layers, while the top-down one refers to exfoliation from bulk MOFs. Different 2D-MOF layers are linked by weak interactions, such as van der Waals forces, π–π stacking and the like. Hence, one can detach MOF layers from bulk MOFs to obtain 2D MOFs. Typically, the top-down strategy usually includes sonication exfoliation and mechanical exfoliation, while the bottom-up one consists of the Langmuir–Blodgett method, modulated synthesis and the like. Typical synthetic strategies are going to be summarized here.

2.1.1 Langmuir–Blodgett method. The Langmuir–Blodgett (LB) method is a feasible method to prepare ordered, large-area, thin nanosheets on the surface of a liquid.[53] The monomers of 2D materials were spread over the surface of a liquid and packed into a dense film, followed by the injection of a metal ion solution.[54] This method could give rise to monolayers or polylayers of MOFs, which makes it a flexible approach to prepare 2D MOFs.

In fact, the LB method is usually combined with the layer-by-layer method to assemble several MOF nanosheets together to form a nanofilm. Makiura *et al.* prepared a series of nanofilms of metal–organic frameworks on surfaces (NAFS) which are composed of 2D MOF nanosheets based on metalloporphyrin linkers and metal ion centres.[55] They assembled copper ions and 5,10,15,20-tetrakis(4-carboxyphenyl)porphyrin (H_2TCPP) molecules to obtain NASF-2. As illustrated in Fig. 2, a 2D MOF is

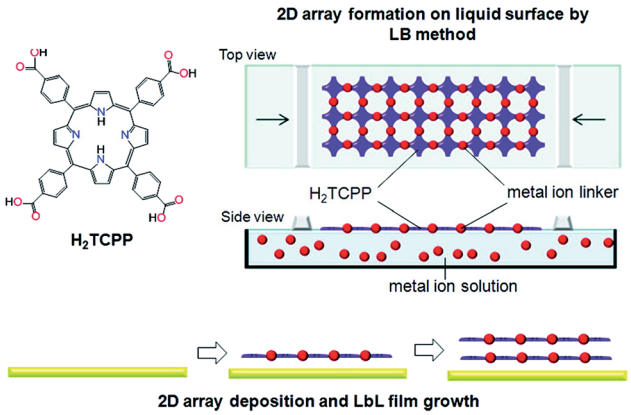

Fig. 2 Illustration of the formation of NASF-2.[55] Copyright 2011, American Chemical Society.

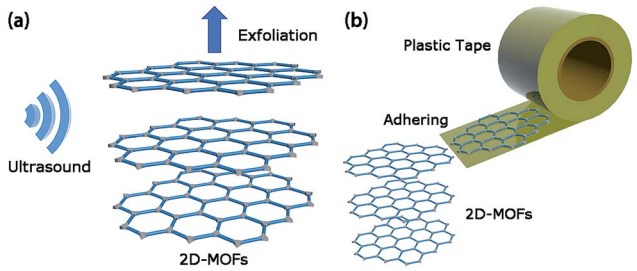

Fig. 3 Comparative illustrations of sonical (a) and mechanical (b) exfoliation methods.

firstly formed on the surface of the solution *via* the LB method, and then a second monolayer is formed to obtain a multilayer nanofilm. The monolayers are assembled by connected water molecules. Actually, NAFS-1 has also been prepared by the LB method earlier.[56] A definite advantage of this method is that, the absence of pillaring units between layers makes the interlayer space tunable. Axially coordinated water molecules could be substituted by suitable components, and the interlayer space could further be controlled. Although this method is employed to prepare nanofilms, obviously it could also result in MOF monolayers.

2.1.2 Sonication exfoliation method. As for 2D-MOF crystals, different layers are connected through weak interactions, including hydrogen bonding as well as van der Waals forces. Provided that the weak interactions are broken, single-layered 2D MOFs could be obtained. And this could be achieved by a concise sonication exfoliation method (or a liquid exfoliation method), which could further lead to 2D-MOF nanosheets.[29] A 2D MOF-2 nanosheet was prepared by the sonication exfoliation method. Dried powder of MOF-2 was sonicated at room temperature to carry out delamination in acetone. Then after the sedimentation of the layered suspension, a colloidal suspension could be obtained. And the 2D MOF-2 nanosheets could be obtained by volatilizing the acetone.[57] Zamora *et al.* deposited sonicated solutions of Cu(I,II) CPs on highly oriented pyrolitic graphite and obtained isolated monolayers.[58] Some other studies preparing 2D MOFs *via* the sonication exfoliation method have also been proposed,[59–61] and an excellent review has been presented about the liquid exfoliation method.[62] In fact, many types of exfoliation methods of bulk materials have been developed, which will be discussed below.

2.1.3 Mechanical exfoliation method. Similar to the sonication exfoliation approach mentioned above, mechanical exfoliation is also an excellent method to prepare 2D materials, including 2D MOFs. The differences between sonical and mechanical exfoliation methods are shown in Fig. 3. Typically, a Scotch-tape method has been used for the exfoliation of graphene or some other materials[63] rather than coordination polymers because of the fragility of crystals. A mechanical exfoliation approach has been reported recently by Espallargas *et al.* They took $[Fe(bimCl)_2]$ (HbimCl = 5-chlorobenzimidazole) for instance, and demonstrated that the mechanical exfoliation method could be extended to almost all 2D materials.[50] Bulk crystals could be exfoliated simply using plastic tape, and the flakes of monolayers could be obtained and observed. This method could be extended to the preparation of almost all 2D coordination polymers.

2.1.4 Modulated strategy. As is known to us all, MOFs could exhibit 3D structures thanks to the noncoplanar multi-coordination of metal ions or organic ligands. In order to obtain 2D MOFs, monodentate ligands could act as a modulator and be employed to react with metal ions to resist the growth of MOF crystals along special directions. This can result in the anisotropic growth of MOF crystals and promote the formation of 2D MOFs.[30] Wang *et al.* employed acetic acid to modulate the growth of a tetragonal crystal MOF, and successfully lead to the anisotropic growth.[64] The acetic acid on the metal ion cluster causes steric hindrance and fewer haptos in a special direction, further statistically leading to the anisotropic growth. Actually, the roles that modulators may play mainly include: (1) controlling the number of haptos on metal ions to control the direction of the growth, (2) causing steric hindrance to result in anisotropic growth, (3) regulating the growth kinetics, and (4) preventing the aggregation of crystals.

Provided that we prefer to obtain single 2D-MOF nanosheets, we could employ monodentate ligands to occupy the noncoplanar haptos of metal ions and leave the coplanar ones, which could further lead to the formation of MOF nanosheets (Fig. 4). We may exploit the trans effect to control the reaction. We could choose monodentate ligands with a stronger trans effect than organic linkers so as to achieve *para* substitution. This strategy could result in 2D MOFs whose original structure is 3D. The varieties of 2D MOFs could be expanded rather than confined to the original MOF nanosheets.

2.2 Various topology of 2D MOFs

The topology of 2D MOFs has been studied in many reports. Traditionally, the topology control of MOFs is achieved by the selection of metal ions, organic linkers and synthetic conditions.[32] We would like to emphasize that, although some 2D networks of MOFs are involved in the formation of layered crystals macroscopically, their monolayer nanosheets could be

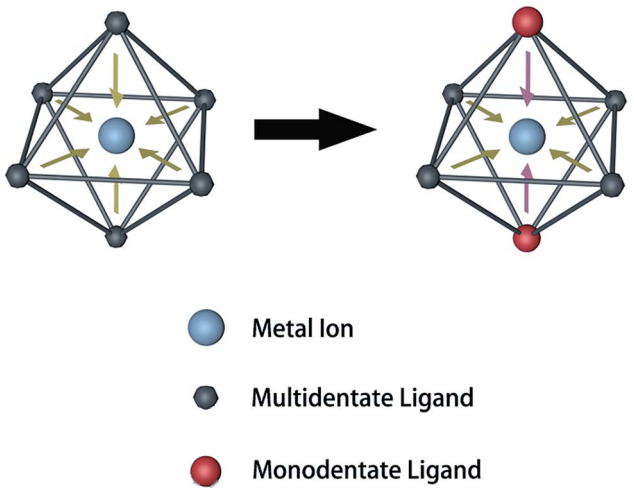

Fig. 4 Illustration of the modulated synthetic strategy.

easily obtained by exfoliation methods mentioned earlier because the layers are packed by van der Waals forces rather than chemical bonds or interpenetration structures. Hence we could regard them as 2D MOFs and discuss their topology. Many studies constructed disperse 2D MOFs by stepwise reactions. Choe *et al.* developed a bridging-linker replacement strategy to obtain special structures.[65] 2D MOFs with a disperse topology can be obtained through many new methods. Unlike covalent-organic frameworks (COFs),[66] MOFs always exhibit a complex topology. Yaghi *et al.* proposed the topology analysis of MOFs, but mainly focused on 3D construction.[67] However, thanks to the coplanar structure, the topology of 2D MOFs is more concise. In a way, it can be explained with the minimal transitivity principle.[67] The planar structure prevents the arrangement of organic linkers in 3D space, and further reduces the types of vertices that the linkers might act as in a net. This may finally cause minimal transitivity of the 2D MOFs, and make their topology more concise. The bridging-linker replacement 2D structures are mostly based on (4,4) or (6,3) topological nets.[68] For example, the first 3d–4f heterometallic framework containing supramolecular 1D channels with a (6,3) topology was reported.[69] A 2D MOF containing equivalent 2D network was also reported, which exhibits a (4,4)-sql topology.[70] We can design different 2D MOFs based on the same topology, although the metal ion clusters and organic linkers could be changed. This strategy is called the isoreticular principle.[71]

Differently, a 2D network $\{[Zn_2(BPBP)(4,4'\text{-sdb})_2]\}_n$ (BPBP = 5,5′-bis(4-pyridyl)-2,2′-bithiophene, and 4,4′-H_2sdb = 4,4′-sulfonyldicarboxylic acid) was constructed, which displays a $\{4^4\cdot6^2\}$-sql topology. The coordination environment of Zn(II) is shown in Fig. 5a, in which the two Zn(II) ions are crystallographically independent. Each Zn(II) ion is coordinated by two symmetrical 4,4′-sdb ligands through four oxygen atoms and a BPBP ligand through one nitrogen atom. A dinuclear Zn(II) "paddlewheel" type SBU is generated by connecting the pairs of Zn(II) ions using the symmetrical 4,4′-sdb ligands. And as Fig. 5b shows, these SBUs are bridged through the second carboxylate groups of the 4,4′-sdb ligands to form a 1D $[Zn_2(4,4'\text{-sdb})_2]_n$ chain containing a 10.25 Å × 13.75 Å loop. Then the 1D $[Zn_2(4,4'\text{-sdb})_2]_n$ chains are connected by BPBP ligands to form a 2D layer with the distance between Zn(II) ions being 18.830 Å (Fig. 5c). Taken together, the sql topology can be shown as in Fig. 5d.[72] Hence the topology of 2D MOFs is related to not only the coordination of groups in the structure, but also the lengths of the groups. The length of ligands plays an important role in the stability of MOF structures. In general, MOFs based on nanoscopic ligands exhibit the tendency to collapse in a vacuum due to the instability of the long ligands after the guest molecules are removed. Some PCNs are constructed from cuboctahedral cages in a (3,24)-connected topology to form microwindows to improve the stability of PCNs.[73]

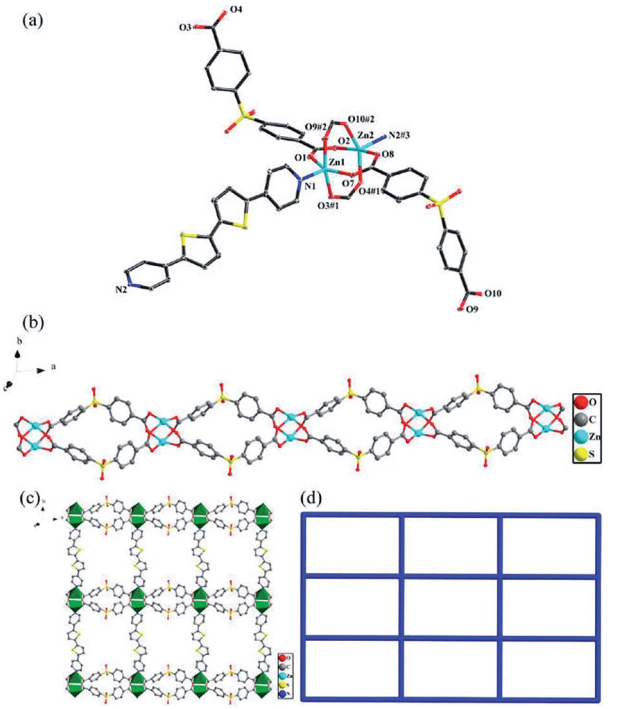

Fig. 5 (a) Coordination environment of Zn(II) ions. The hydrogen atoms are left out in view of clarity. (b) The 1D chain composed of 4,4′-sdb ligands and Zn(II) ion centers. (c) The structure of the 2D MOF. (d) The sql topology of the 2D MOF.[72] Copyright 2013, American Chemical Society.

An important tool to study the topology of MOFs is their simplified underlying net.[71] Taking the MOF in Fig. 5c as an example, the atoms are apparently not coplanar; however, the propagation direction of the crystal is in a plane (along the *a*- and *b*-axes in the crystallographic plane), and the crystallographic planes are linked by secondary bonds rather than chemical bonds. Hence, it should be regarded as a type of 2D MOF. Actually, the structure of 2D MOFs may not necessarily require the coplanarity of all atoms, such as the structure in Fig. 5c. Hence, we may define that, a type of MOF, so long as its simplified underlying net is in the same plane, can be called a 2D MOF.

Based on the topology of 2D MOFs, one can choose appropriate metal ions and organic ligands to construct the target MOFs. Many potential factors, such as the coordination number of metal ions and the length of ligands should be taken into account. For 2D MOFs, the haptos of ligands should be in the same plane to ensure that the subsequent MOFs have a 2D structure, or, according to our aforementioned discussion in 2.1.4, appropriate monodentate ligands should be introduced in order to control the growth of MOFs in special directions.

2.3 Relationship between 2D and 3D MOFs

In some cases, lots of 3D MOFs could be regarded as the assembly of 2D MOFs. 3D MOFs could be split to 2D MOFs in order to study their structures and topology. Thus, we are going to discuss the relationship between 2D and 3D MOFs. Actually, apart from the 3D structure connected by coordinated small molecules we have mentioned in Section 2.1.1,[55] many connection styles are also developed. A 2D MOF can be formed into a laminated form by inter-layer π–π interactions to construct a 3D MOF.[74] According to a previous report, $[Zn_{10}(BBC)_5(BPDC)_2(H_2O)_{10}](NO_3)(DEF)_{28}(H_2O)_8$ (DUT-43) was prepared under solvothermal conditions, where BBC = 4,4′,4″-(benzene-1,3,5-triyl-tris(benzene-4,1-diyl))tribenzoate and BPDC = 4,4′-biphenyldicarboxylate. It has a 3D structure, which is formed by two kinds of 2D MOFs. One is a kind of honeycomb layer composed of structural units and based on BBC as an organic linker; the other is composed of three honeycomb layers which are connected by BPDC. The simplified three-dimensional structure has been given (Fig. 6a), which shows the three-dimensional structure of the two three-layer structures interspersed by a single-layer structure.[75] Similarly, $[Cu_4(TPOM)_2L_4]\cdot 3H_2O$ (H_3L = 1,3,5-benzenetricarboxylic acid and TPOM = tetrakis(4-pyridyloxymethylene)methane)[76] can also form 3D networks.

Apart from the inter-layer π–π interactions, organic linkers could also join 2D layers together to form 3D MOFs. A 3D MOF, $[Co_2(TCTA)(BPY)_2(H_2O)_4]_n$ (H_4TCTA = *p-tert*-butyl-thiacalix[4]arene tetraacetic acid, BPY = 4,4′-bipyridine), was constructed from 2D sheets, which are connected by TCTA (Fig. 6b).[77] The two formations to construct 3D MOFs from 2D structures could be extended to the construction of other frameworks.

Interpenetration is also an important formation of the construction of 3D structures from 2D MOFs. The interpenetration in 2D structures has been reviewed earlier. According to the earlier review, parallel and inclined interpenetration are two types of interpenetration between 2D layers.[68] A $\{[Cd_2(oba)_2(IP)_2(H_2O)]\cdot H_2O\}_n$ (**1**, H_2oba = 4,4′-oxybis(benzoic acid), and IP = 1*H*-imidazo[4,5-*f*][1,10]-phenanthroline) compound was prepared, which exhibits a parallel interpenetrating structure (Fig. 7a).[78] Two 2D-MOF sheets in **1** are displayed in Fig. 7a, which are on the left side and right side, respectively. The 2D-MOF sheets stack alternately and could finally form a 3D structure. A Co{[HBDC][$BDC]_{0.5}$[INH]} (**2**, BDC = 1,4-benzenedicarboxylic acid, and INH = isonicotinylhydrazine) 2D coordination polymer also exhibits an interpenetrating structure (Fig. 7b),[79] which is constructed by interpenetration of closed paths. The Schläfli symbol of **2** is 6^3. The interpenetration provides the structure of **2** with higher thermal stability. In fact, 3D MOFs can also exhibit interpenetrating structures.[80]

The discussion about the relationships between 2D and 3D MOFs is helpful for the synthesis of 2D MOFs. As is emphasized in the previous section, 2D MOFs could be exfoliated from 3D MOFs which are composed of monolayers to obtain MOF nanosheets. There are mainly four connection styles, namely (1) small molecule connection (intermolecular force), (2) inter-layer π–π interacting connection, (3) organic linker connection, and (4) interpenetrating connection. Obviously, an exfoliation method is not suitable for the latter two connection styles for the sake of the strong combining ability of covalent bonds in the 3D network. Hence, exfoliation methods could only be applied to the 3D MOFs constructed by intermolecular force or π–π interacting connection.

2.4 Applications of 2D MOFs

2D MOFs, also known as MOF nanosheets, frequently exhibit impressive nano effects. On the edge of 2D MOFs, lots of unsaturated active sites endow them with high reactivity or responsive activity, which is called the surface effect. And the planar structure of the nanosheet leads to a conjugation system, which further allows electron delivery on the nanosheets. 2D MOFs have wide application in sensors, conductive devices, switch devices[81] and so on. In view of typicalness, here we mainly introduce the application of 2D MOFs in sensors, conductive devices and catalysis.

2.4.1 Sensor. Recently, the selective and sensitive detection of gaseous mixtures is in great need.[82] Gas sensors have a great influence and a wide range of applications, which include

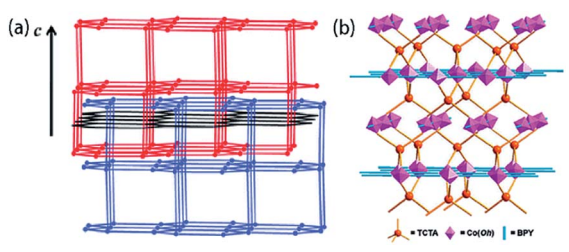

Fig. 6 3D MOFs constructed from 2D sheets by (a) inter-layer π–π interactions.[75] Copyright 2012, Royal Society of Chemistry. And (b) organic linkers.[77] Copyright 2011, American Chemical Society.

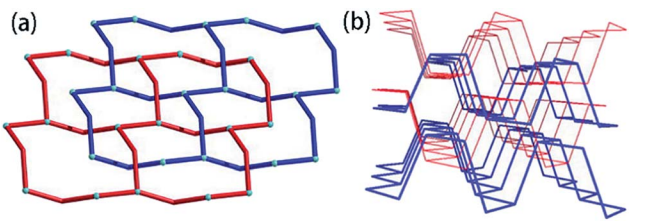

Fig. 7 The interpenetrating structures of (a) **1**[78] (copyright 2012, Elsevier) and (b) **2**[79] (copyright 2013, Elsevier) respectively.

industrial process management, food quality control, environmental monitoring, chemical threat detection, occupational safety, and medical diagnostics.[83–86] The rich host–guest chemistry and porous structures that respond to external stimuli of MOFs have attracted much attention of researchers for the development of biological and chemical sensors.[87,88] In fact, many kinds of MOFs can be used as sensors, not only for gas monitors, but also for other applications, due to their photochromic, electrochromic, photoluminescence, electroluminescence and other characteristic responses. As is well known, 2D nanosheets could exhibit special nanoeffects. Their sufficient unsaturated active sites and planar structure are convenient for the stimulation and deliver of electrons. This further enable them to be used in sensors. Based on 2D MOFs, many research studies have been conducted aimed at the application of MOFs as sensors.

The MOFs with photochromic or electrochromic properties can be applied in photoelectric conversion devices. NBU-3 is the first 2D MOF with both electrochromic and photochromic properties. The photochromic process is reversible, changing between yellow and dark green. This type of discovery can be used in the fields of memory materials and photoelectric conversion.[3]

NUS-1a which displays responsive turn-on fluorescence to many volatile organic compounds has been reported. It is an activated analogue of 2D layered NUS-1. It could be obtained by evacuating the crystal of NUS-1 to remove the solvent molecules in the crystal. The sensing study was carried out by immersing NUS-1a in different volatile organic compounds followed by photoluminescence tests. Compared with the pristine crystals, NUS-1a immersed in benzene exhibited a red shift, and the crystal soaked in mesitylene exhibited a blue shift. The relationship between fluorescence emission and the emission wavelength is displayed in Fig. 8. According to previous literature, a coplanar conformation can promote π electron conjugation, which further leads to a red shift, while a perpendicular conformation can weaken π electron conjugation which further results in a blue shift.[89,90] When NUS-1a is exposed to analytes, the conformation of the dangling phenyl rings might be changed. This further leads to the peak shifts of the electrons. Interactions between the dangling phenyl rings of NUS-1a and analytes could impede the rotation and/or vibration of the phenyl rings and further hinder trigger peak shifts as well as the responsive turn-on fluorescence. NUS-1a could be used as the sensor for various volatile organic compounds and might further find wide application in sensing.[91]

2.4.2 Conductive devices. Most of the current research is mainly focused on the application of MOFs in catalysis, separation and gas storage. In fact, MOFs can also be used in the field of electronic devices.[92–94] However, the poor conductivity of MOFs limits their uses in batteries, fuel cells and many other applications.[95] Thus, the design and modification are needed. Fortunately, the rigid or flexible structures of MOFs enable them to be tuned to reach a higher conductivity.[96] The incorporation of satisfactory magnetic and/or electrical properties into a MOF requires embedding these materials into nanosheets, which can prepare transparent and flexible electronic and/or optoelectronic devices or functional membranes and molecular sieves.[97] The crystal engineering strategy can help us design the structure of MOFs *via* the selection of organic linkers and metal ion clusters. Actually, the preparation of MOFs into nanoflakes can optimize their electrochemical performance, in which MOFs remain highly crystalline and porous, with increased specific capacitance.[6,98] As mentioned earlier, the planar conjugated structure of 2D MOFs endows them with high electron conductivity. Lots of studies have been carried out to develop conductive devices based on 2D MOFs.

A 2D cobalt 2,3,6,7,10,11-triphenylenehexathiolate framework has been reported, which exhibits temperature-dependent charge transport properties. The temperature-dependent resistivity of the 2D MOF was measured on a pressed pellet of the 2D MOF with various thicknesses. According to the measurement results, it exhibits a pronounced temperature-dependent resistivity and a strong correlation between the transition temperature and film thickness (Fig. 9). According to the authors, the

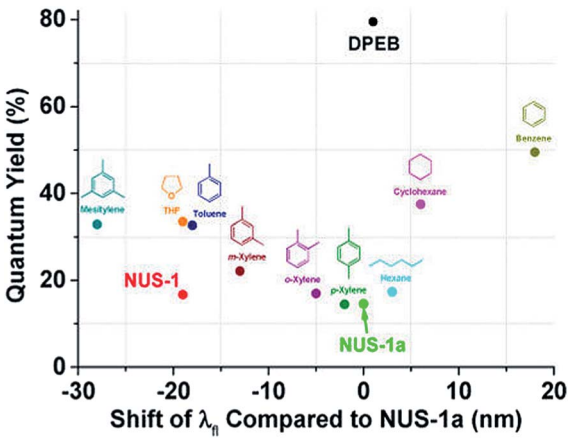

Fig. 8 The fluorescence emission spectra of NUS-1a in different volatile organic compounds.[91] Copyright 2014, American Chemical Society.

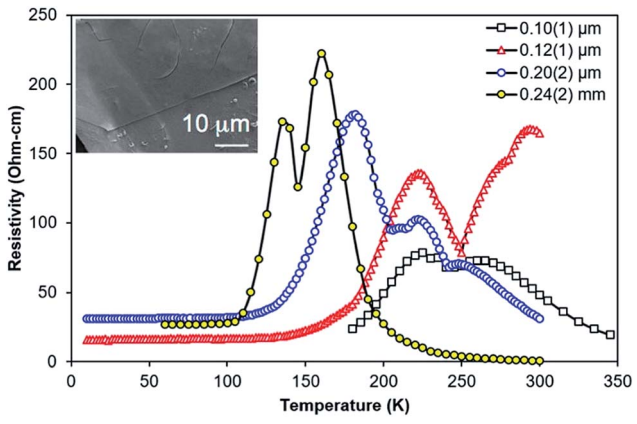

Fig. 9 The variable-temperature resistivity measurement for the 2D-MOF material. Inset in the panel shows the SEM image of the 2D-MOF material.[99] Copyright 2017, American Chemical Society.

changes of conductivity of the 2D MOF might be due to the changes in the interlayer spacing, vibrational modes and morphology, which could be influenced by temperature.[99]

The Seebeck effect describes the relationship between the difference in temperature and current. The Seebeck effect has been observed in some 2D MOFs. 2D MOFs $X_3(HITP)_2$ (X = Ni, Pt or Pd, and HITP = 2,3,6,7,10,11-hexaiminotriphenylene) has been reported, which have large Seebeck coefficient values of 600 μV K^{-1} at room temperature.[100] This impressive performance makes 2D MOFs potential temperature sensors.

The requirement of novel semiconductor materials is increasing due to the miniaturization of the feature sizes of the integrated circuits as well as the development of the semiconductor industry. Particularly, MOFs could be a potential candidate for new semiconductor materials in microelectronics, although the integration is still at an early stage of development. As for 2D MOFs, lots of semiconductor materials have been developed. Su *et al.* developed a calcium-based 2D MOF by a solvothermal method.[101] In this study, a dual-channel emitting pathway theory was proposed. In the 2D MOF prepared in this study, the energy emission below 500 nm could be attributed to the interlayer trapped excitons by 2D layers after charge transfer while the energy emission above 500 nm could be imputed to intralayer formed excimers. The emissions exhibit an excitation-dependent shifting tendency. For low energy excitation (excitation wavelength = 460–530 nm), the dominant energy emission is above 550 nm; at an excitation wavelength of 420–450 nm, a pronounced long wavelength emission above 550 nm was observed; and at an excitation wavelength of 265–408 nm, an apparent emission which shifts from 430 to 470 nm could be observed. This excitation-dependent shifting tendency allows the 2D MOF to be used in the semiconductor field.

2.4.3 Catalysis. Typically, the catalytic properties of MOFs attract much attention from researchers. Lots of reactions can be promoted by MOFs and their derivatives efficiently. Thus, it is vital to study the design of MOF catalysts. The catalytic properties of MOFs strongly depend on the nature of the metal ion clusters as well as the additional organic linkers.[102] Hence the selection of metal ions and organic linkers is very important. Especially, indium[102] and some transition metal ions exhibit considerable catalytic activity. As for organic linkers, a conjugated system is useful for the improvement of catalytic activity. In view of this, different combinations of metal ions and organic linkers can be developed to obtain efficient catalysts. Benefiting from the sufficient active sites and large conjugated structures, 2D MOFs exhibit impressive catalytic performances.

High-standard electrocatalysts are greatly required in many energy storage and conversion systems.[103–105] In many ways, electrocatalysis of the hydrogen evolution reaction (HER), oxygen evolution reaction (OER) and oxygen reduction reaction (ORR) is vital for the solution of energy shortage and environmental pollution. Hence, the search for effective electrocatalysts is an important topic. 2D cobalt 1,4-benzenedicarboxylate (CoBDC) and $Ti_3C_2T_x$ nanosheets were combined through an interdiffusion reaction-assisted strategy, and the composite is denoted as $Ti_3C_2T_x$–CoBDC. $Ti_3C_2T_x$–CoBDC exhibits an electrocatalytic activity for the OER, which shows a Tafel slope of 48.2 mV dec^{-1} at a current intensity of 10 mA cm^{-2} and an onset potential of 1.51 V (*vs.* RHE).[106] In order to introduce more hydrogen active sites into 2D MOFs to improve the catalytic activity of 2D MOFs towards the HER, metal bis(diamine) (MN_4, M = Co and Ni), metal bis(dithiolene) (MS_4) and molecular metal dithiolene–diamine (MS_2N_2) complexes were incorporated into carbon-rich 2D MOFs. They act as electrocatalysts for the HER during the process. The combination of nitrogen, sulfur and metal synergistically facilitated the adsorption/desorption of H_2. In this study, the operating potential of Co dithiolene–diamine coordination was found to be 283 mV at 10 mA cm^{-2}, and the Tafel slope was found to be 71 mV dec^{-1}, indicating an excellent electrocatalytic activity towards the HER.[54]

2D MOFs could also be used as catalysts for organic reactions because they can act as a Lewis acid. A 2D framework, $[Sc_2(pydc)_3(H_2O)_4]\cdot 5H_2O$, was synthesized from 2,3-pyridinedicarboxylic acid (H_2pydc) and Sc(III) ions. The 2D MOF exhibits excellent catalytic activity for the cyanosilylation of *p*-nitrobenzaldehyde in acetonitrile. With this 2D MOF, the conversion of *p*-nitrobenzaldehyde was reported to be 99% after 90 minutes of reaction, indicating the excellent catalytic properties of the 2D MOF. The pronounced Lewis acid catalytic effect of the 2D Sc-based MOF could be attributed to the electron-unsaturated Sc(III) metal sites, which lead to its high electronic reception capability.[107] Hence, the selection of metal ions to construct a 2D MOF could remarkably influence the catalytic activity of the 2D MOF, and the 2D MOFs based on unsaturated metal ions could act as electrophilic reagents in organic reactions. Two highly active species obtained from the 2D Co-based MOF exhibits high catalytic activity towards the transformation of biomass-derived furfural, which also indicates the important role that the open metal centres play in organic reactions.[108]

2.4.4 Precursor of nanoparticle doped carbon nanosheets. Some derivatives of 2D MOFs also exhibit enhanced catalytic performances. Dong *et al.* reported an *in situ* synthetic strategy of ultrathin ZIF-67 nanosheets with a salt-template, and the nanosheets are carbonized to prepare Co/N co-doped carbon nanosheets (Co, N–C NSs) which exhibit electrocatalytic activity towards the ORR. NaCl powder and a methanol solution of MeIm and $CoCl_2$ were mixed under stirring so as to obtain ZIF-67 nanosheets. Then the methanol solvent was evaporated and Co, N–C NSs were obtained through *in situ* pyrolysis. The brief illustration of the preparation process is shown in Fig. 10a. Different Co, N–C NSs were caused by different pyrolysis temperatures, and are denoted as Co, N–C NS-T °C where T refers to 600, 700, 800 or 850. Meanwhile, a Co/N co-doped carbon nanoparticle denoted as Co, N–C NP-800 °C was prepared from rhombic dodecahedral ZIF-67 nanocrystals for comparison. The electrocatalytic activities of different samples towards the ORR were studied. According to Fig. 10b, Co, N–C NS-800 °C exhibits the highest current density and the most positive onset potential as well as halfwave potential among the Co, N–C NS samples, indicating the enhanced ORR activity of Co, N–C NS-800 °C. And as shown in Fig. 9c, Co, N–C NS-800 °C

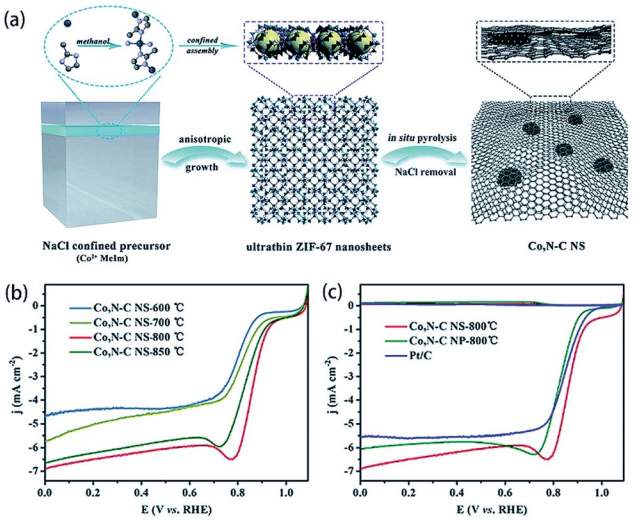

Fig. 10 (a) Illustration of the synthesis process of ZIF-67 nanosheets as well as Co, N–C NS derived from ZIF-67 nanosheets. (b and c) Linear scanning voltammetry curves of different Co, N–C NSs, Pt/C and Co, N–C NP-800 °C.[109] Copyright 2017, Royal Society of Chemistry.

exhibits a halfwave potential of 0.869 V, which is more positive than that of Co, N–C NP-800 °C (0.832 V) and Pt/C (0.846 V), which suggests the enhanced electrocatalytic activity of Co, N–C NS-800 °C.[109] This study suggests that effective electrocatalysts could be obtained from the derivatives of 2D-MOF nanosheets.

3. MOF membranes

In recent years, MOF membranes have attracted much attention from researchers due to their excellent gas separation capacity, considerable catalytic properties and so on. However, there are still many challenges in these fields. Regarding controllability, although many MOF membranes exhibit separation capacity, the modification of their structures as well as functionality is still a great challenge.[33]

As for application aspects, industrial gas mixtures are often multi-component systems. If it is desired to selectively separate a certain gas from a mixed gas through a MOF membrane, this membrane should be required to have a good selective adsorption function; however, the selectivity of many MOFs cannot meet this demand.[33] Besides, many MOF membranes have poor proton-conductivity capacities, so they should be prepared based on conductive substrates.[110] However, according to relevant reports, the influence of the matrix on the properties of the membranes is stronger than that of the MOF itself. MOF membranes with better gas selectivity tend to adhere to inorganic substrates, which are relatively expensive. We hope that the MOF layer can be built on porous polymers, but the realization of this goal is still limited by technology.[111] The main restriction is the poor combination force between substrates and MOF membranes.[110] Recently, many excellent reviews have been published, which summarized the structure, design, construction and application of MOF membranes.[112–117] Here we choose to introduce MOF membranes with respect to synthetic methods as well as applications.

3.1 Synthetic methods of MOF membranes

About 10 years ago, the construction technology of MOF membranes nearly hadn't been developed,[118] but great progress has been made in a decade. We mainly summarize the reports of MOF membranes divided according to synthetic strategies. Especially, because various synthetic strategies of MOF membranes have already been developed, we are going to organize this section by the classification of their synthesis methods, and the experimental methods are introduced below.

3.1.1 Solvent method. The solvent method is the most common strategy for the preparation of MOF membranes. Typically, precursor solutions are mixed and the reaction is carried out under heating or at room temperature, followed by filtration to obtain MOF membranes. In fact, lots of strategies which will be discussed later are based on the solvent method (*i.e.*, spin rotation method). The solvothermal method is a kind of solvent method. In the solvothermal method, the substrate is preliminarily placed in a reaction solution, and the solution is heated. Sometimes it is necessary to preheat the reaction solution. The solvothermal method can lead to thinner MOF membranes.[119] In detail, the solvothermal method includes two strategies, namely *in situ* method and secondary growth.[120] The *in situ* synthesis method could lead to substrate corrosion and the lack of control to prepare a homogeneous coating; however, the secondary growth requires nano-sized MOF seeds.[121] Sometimes, the surface of the substrate can be modified with hydroxyl, carboxyl or other functional groups in order to increase the bonding strength between MOF films and the substrate.[122] However, though the solvothermal method is a classical strategy to obtain MOF membranes, there are still a lot of obstacles in the development of this method: (1) control of the synthesis and growth of membranes can be difficult to implement, which results in thick MOF membranes; (2) the cracks between the substrates and membranes may cause different thermal expansion coefficients if the reaction system is cooled back to room temperature; and (3) the prohibitive cost limits its large-scale application.[123] The synthetic methods of MOF membranes should be able to improve their separation performance. Appropriate MOFs and matrices have been chosen to construct MOF membranes and many strategies have been developed.

Typically, ZIF-9 can be synthesized from $Co(NO_3)_2 \cdot 6H_2O$ and benzimidazole (bIM), while ZIF-67 from $Co(NO_3)_2 \cdot 6H_2O$ and 2-methylimidazole (mIm). Zhang *et al.* synthesized a ZIF-9-67 membrane which is based on ZIF-67 and ZIF-9 from $Co(NO_3)_2 \cdot 6H_2O$, bIM and mIm. In this research, α-Al_2O_3 was used as a matrix. The ZIF-9-67 membrane exhibits great selectivity for CO_2 separation (Fig. 11). According to Fig. 11a, CO_2 has the lowest permeance value among various gases, and it has a different behavior from other gases. An increase appears when temperature is higher than 330 K. The ZIF-9-67 membrane exhibits great selectivities for a mixture of CO_2 and other gases, especially H_2 (Fig. 11b). The ideal separation factor of CO_2–H_2

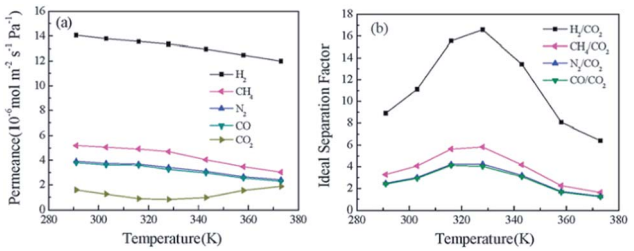

Fig. 11 (a) The permeance of different gases at various temperature; (b) ideal separation factor of different gases at various temperatures.[33] Copyright 2013, Royal Society of Chemistry.

reaches nearly 16, indicating the considerable separation capacity of the ZIF-9-67 membrane.[33]

Knebel *et al.* successfully prepared a 200 nm UiO-66 membrane deposited on an α-Al_2O_3 substrate. Azobenzene (AZB) is loaded in the pores of the UiO-67 membrane. The control of CO_2 permeability and H_2/CO_2 separation based on AZB-loaded UiO-67 membranes were tracked by *in situ* irradiation and permeation. Changes in external conditions can switch the gas composition. This resulted in an ultrathin smart UiO-67 membrane. The permeability of this UiO-67 membrane to a single gas and the permeability of the AZB-laden UiO-67 membrane to a gas mixture are shown in Fig. 12.[119]

Flexibility is an important feature for the usefulness of the material in many applications.[124,125] Most MOFs are structurally flexible, which promotes their application in various fields.[86,126] Hence it is vital to embed MOF membranes into flexible substrates to retain the flexibility. Nanofibrous mats can also be used as a perfect substrate for the growth of MOF membranes because of their large porosity, high specific surface area, and enormous structural as well as chemical tunability. Wu *et al.* reported the fabrication of several MOF membranes with electrospun nanofibrous mats being used as the substrate. HKUST-1, ZIF-8, $Zn_2(bpdc)_2(bpee)$ (bpee = 1,2-bipyridylethylene) and MIL-101(Fe) are fabricated *via* this method. Two steps are included during the modification, which are the impaction of MOF crystal seeds and the integration of MOF crystals, respectively (Fig. 13). The crystal seeds can be embedded *via* the solvothermal method. And the integration of MOF crystals can be implemented by dropping the MOF precursor solution under applied voltages. By this modification, MOFs can be embedded into flexible substrates and be used in flexible devices.[127]

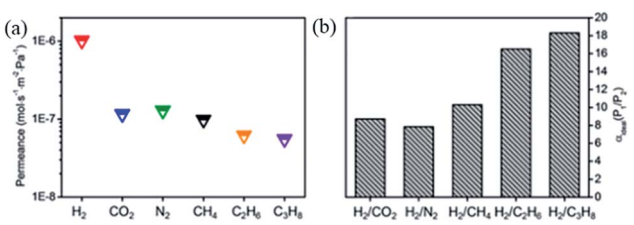

Fig. 12 (a) The single-gas permeances; (b) the ideal permselectivities of different gas mixtures.[119] Copyright 2017, Royal Society of Chemistry.

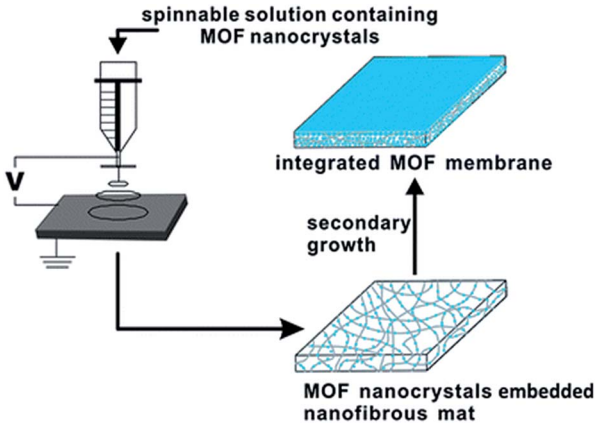

Fig. 13 Scheme of the electrospun nanofibrous mats used as the substrate for MOF membranes.[127] Copyright 2012, Royal Society of Chemistry.

Jeong *et al.* modified an IRMOF-1 membrane with a surfactant in order to avoid fractures and cracks in the membrane during the drying process.[128] The surfactant can reduce interfacial tension, which represses the formation of cracks as well as fractures. An IRMOF-1 membrane was also prepared by the solvothermal method in their study.[129] Heptanoic anhydride (AM6) was used to modify the membrane. The IRMOF-1 membrane was immersed in a chloroform solution of AM6 to complete the modification. Then the membrane was kept in a chloroform solution of Pluronic P123 or Span 80 (Sorbitan oleate). After these processes, the membrane was dried without the generation of any fractures or cracks.

Different from the traditional strategy of preparing a membrane by directly mixing a metal ion solution, an organic linker solution and a substrate, Livingston *et al.* used two methods to prepare HKUST-1 on Polyimide P84 supports. Traditionally, *in situ* synthesis refers to the preparation of a HKUST-1 film by directly mixing an aqueous solution of copper acetate, a solution of H_3BTC in octanol, and the substrate. And Livingston *et al.* proposed two different facile strategies. Scheme A indicates that the substrate can be first soaked in the aqueous solution of copper acetate for a period of time. After the substrate is taken out, the solution of H_3BTC in octanol is poured on the surface of the substrate. In contrast, in Scheme B, the substrate is first used in the H_3BTC solution. Then the aqueous solution of copper acetate is used. The HKUST-1 film synthesized by Scheme A is mainly located on the surface of the substrate, while the HKUST-1 film prepared by Scheme B is embedded on the surface of the substrate. The solute retention of the composite membrane prepared by Scheme A is about the same as that of the composite membrane obtained by the *in situ* synthesis method, but its permeance value is more than 4 times as much as that of the latter.[130]

Interestingly, Coronas *et al.* synthesized ZIF-7 and ZIF-8 membranes on the inner-side of polysulfone (PSF) *via* pumping reaction solution through the PSF hollow fiber, which exhibits gas separation capacity. This strategy could be developed and expanded to adsorption and catalysis fields.[131]

Many efforts have been made to optimize the formation of MOF membranes on substrates. Especially, according to a previous report, sonication can clean the sample,[132] reduce the size of MOF crystals and improve the affinity to substrates.[133] Zhu *et al.* synthesized HKUST-1 membranes based on poly(2,6-dimethyl-1,4-phenylene oxide) (PPO) with the assistance of sonication. They prepared HKUST-1 membranes which are named CuBTC-S1/PPO (under the sonication of 40% amplitude), Cu-BTC-S2/PPO (under the sonication of 100% amplitude), and Cu-BTC-p/PPO (without the assistance of sonication). Fig. 14 shows the SEM images of the PPO membrane and the composite membranes incorporated with HKUST-1. As shown in Fig. 14b, the Cu-BTC-p/PPO membrane exhibits some voids between Cu-BTC and the substrate, while the PPO membrane exhibits a smooth surface (Fig. 14a). According to Fig. 14c and d, smaller Cu-BTC crystals are generated by sonication treatment, and CuBTC-S1/PPO and Cu-BTC-S2/PPO show a crater-like morphology.[133] Additionally, sodium formate treatment in the synthesis process deprotonates the reaction system.[134–136] It gives rise to uniform distribution of MOF crystals in all directions and finally leads to continuous well-intergrown membranes.[136]

Sonication was also used by Vankelecom *et al.* to construct NH_2-UiO-66-ABA (ABA = 4-aminobenzoic acid).[137] However, they also pointed out the essential role the amine group plays in the formation of a stable membrane. A composite membrane based on NH_2-UiO-66-ABA and Matrimid 9725 was prepared, and the amine group on the outer surface of the MOF moiety results in covalent linking, which contributes to the stable membrane.[138,139]

Apparently, the solvent method is concise in technology and independent of special devices. It could lead to well-crystalline and homogeneous MOF membranes. It might be the most potential method for the manufacture of MOF membranes and thin films. However, as the most common strategy, the solvent method might cause some defects in membranes. Additionally, compared with some novel strategies, the solvent method is difficult to endow the MOF membranes with specific functions. According to the aforementioned strategies, surfactant- and ultrasonic-assisted solvent methods could be employed to overcome these disadvantages, and some other methods have also been developed.

3.1.2 Contra-diffusion method. In order to achieve well-intergrown ZIF membranes, it is vital to achieve the heterogeneous nucleation of MOFs on substrates. Many strategies have been developed, such as the modification of the surfaces of substrates as well as the addition of crystal seeds on supports. However, these strategies usually complicate the membrane synthesis.[140] Researchers have developed a contra-diffusion method to synthesize MOF membrane and films. Briefly, two precursor solutions are placed at both ends of the substrate, respectively, and the solutions each contain one reactant and the same solvent. The two solutions diffuse in opposite directions through the substrate. When the two solutions meet, a ZIF-8 membrane or film can be generated.[111,141,142] Previously, ZIF-8 membranes have been synthesized on polymer substrates, such as bromomethylated poly(2,6-dimethyl-1,4-phenylene oxide)[141] and poly-thiosemicarbazide,[111] in order to avoid the disadvantage of using inorganic substrates. Jeong *et al.* prepared a ZIF-8 membrane on a porous α-alumina support *via* this method, and obtained excellent separation properties for propylene/propane. And the composite is denoted as ZIF-8/α-Al_2O_3.[140] Particularly, MOF membranes can grow on the inner side of hollow fibers by employing the contra-diffusion method. This approach is convenient to control and helpful for the scale-up fabrication of MOF membranes.[143] In another report, ZIF-8 and HKUST-1 were grown on either the inner or the outer surface of polybenzimidazole based hollow fibers (PBI-BuI-HF) *via* the contra-diffusion method. The sketch maps of the synthetic strategy are shown in Fig. 15b. $Zn(NO_3)_2$ was dissolved in water and circulated through the inner side of the fibers, and 2-methylimidazole (2-mIm) was kept on the outer side of the fibers to prepare the ZIF-8@PBI-BuI-In composite. Conversely, one can inject the solution of 2-mIm into the inner side of the fiber, while inject the solution of $Zn(NO_3)_2$ to the outer side.

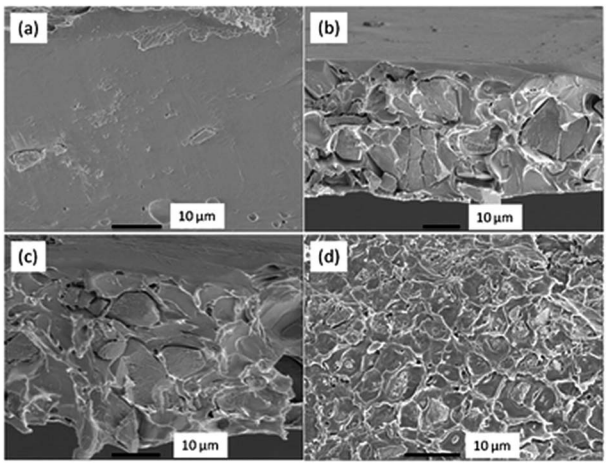

Fig. 14 SEM images of different samples, which are (a) the PPO membrane, (b) Cu-BTC-p/PPO, (c) Cu-BTC-S1/PPO, and (d) Cu-BTC-S2/PPO.[133] Copyright 2013, Royal Society of Chemistry.

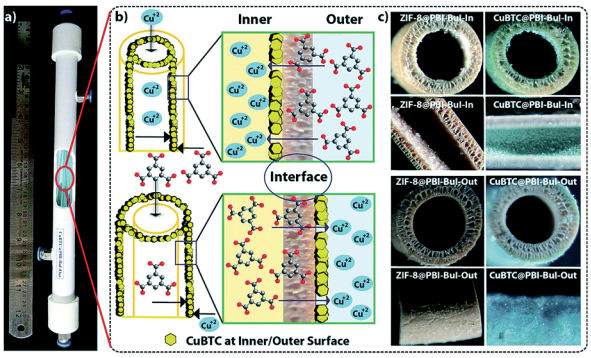

Fig. 15 (a) The photograph of the CuBTC@PBI-BuI-Out composite. (b) The sketch maps of the synthetic scheme of CuBTC@PBI-BuI-Out as well as CuBTC@PBI-BuI-In. (c) Microscopic images of different composites based on PBI-BuI-HF.[144] Copyright 2015, Royal Society of Chemistry.

Then the ZIF-8@PBI-BuI-Out could be obtained. And the same process is used to prepare HKUST-1@PBI-BuI-In and HKUST-1@PBI-BuI-Out. The microscopic images of the composites in this study are shown in Fig. 15c, displaying well-decorated hollow fibers.[144] The contra-diffusion method could lead to MOF membranes embedded into matrixes, further resulting in a strong combination between MOF membranes and substrates. However, the matrices of this method are limited to the ones with high permeability.

3.1.3 Rapid thermal deposition method. The traditional MOF membrane preparation methods are mainly *in situ* synthesis and secondary growth, which are limited by their low reproducibility and scalability and high manufacturing cost. Shah *et al.* used the rapid thermal deposition (RTD) method to prepare a MOF membrane.

Actually, the RTD method is more similar to the liquid phase evaporating (LPE) method, which will be discussed in the MOF Films section. Typically, the main difference between RTD and LPE methods lies in the treatment of the matrix. After the matrix is treated (*i.e.* soaked or slid-coated), for the RTD method, the matrix would be heated and the solvent evaporates; however, for the LPE method, the matrix might be cooled to promote the crystallization of the MOF. The difference is illustrated in Fig. 16. In the RTD method, the solution is driven from the inside of the porous matrix to the outside. At this point, crystallization will occur both outside and inside the matrix. RTD is used to prepare the membranes of ZIF-8 and HKUST-1. The gas permeability is significantly different from that of the membrane prepared by the conventional method (Fig. 17), making it more suitable for gas separation.[145] This method could lead to MOF membranes spread evenly both outside and inside the matrix.

3.1.4 Interfacial synthesis method. Zhu *et al.* have reported a new Interfacial Polymerization (IP) method which can help synthesize thin-film nanocomposite (TFN) membranes. They deposited ZIF-8 on polyacrylonitrile UF membrane (PAN) substrates. The PAN substrates are sequentially immersed in sodium hydroxide solution and deionized water to modify the substrate to obtain HPAN. At the same time, ZIF-8 is modified with poly(sodium 4-styrenesulfonate) (PSS) to be hydrophilized to obtain mZIF. It can be evenly distributed in water (Fig. 18a). The polymerization process can be implemented *via* following steps (Fig. 18b). This facilitates the mixing of ZIF-8 with other hydrophilic reactants. The mZIF is dispersed in an aqueous solution of piperazine. Subsequently, the above suspension is poured on the substrate for particle deposition. The substrate is

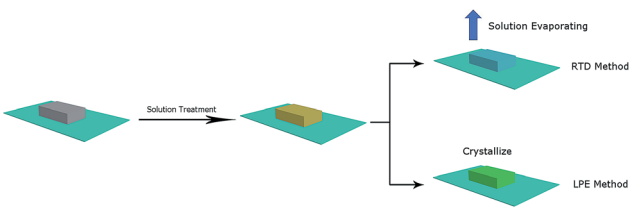

Fig. 16 Illustration of RTD and LPE methods.

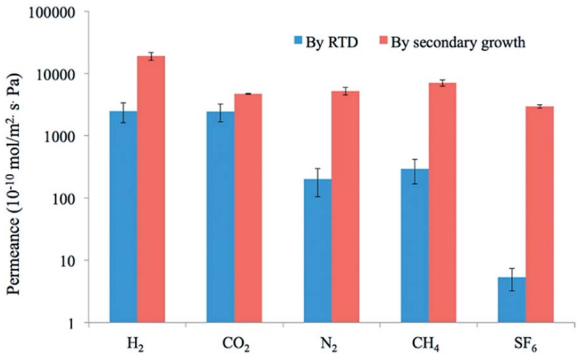

Fig. 17 Gas permeances of HKUST-1 membranes prepared by RTD and traditional methods (secondary growth).[145] Copyright 2013, American Chemical Society.

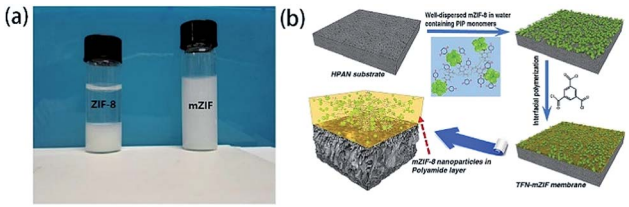

Fig. 18 (a) Comparison of aqueous suspensions of ZIF-8 and mZIF nanoparticles. (b) Scheme of synthesis of TFN containing mZIF nanoparticles *via* the IP method.[146] Copyright 2017, American Chemical Society.

immersed in a solution of trimesoyl chloride (TMC) in *n*-hexane for a period of time, followed by warming to further polymerize. Using this method, a TFN-mZIF membrane can be made. Because of the hydrophilicity of mZIF, the TFN-mZIF membrane can be used as a nanofiltration membrane for aqueous solution.[146] ZIF-11 and MIL-101(Cr) were embedded in the same membrane by IP of polyamide (PA), according to a previous report, in order to combine their different textural and chemical properties.[147] Interfacial growth methods have also been used by other research,[148] which leads to a free-standing conductive MOF membrane.

3.1.5 Postsynthetic polymerization method. Another strategy that can avoid cracks in MOF membranes is the photoinduced postsynthetic polymerization method, according to a previous report.[149] In general, nanocrystals of MOFs are firstly prepared, followed by their modification (for instance using polymers) which endows them with polymeric activity.

Then the nanocrystals are polymerized together under some special treatment (such as ultraviolet light) and form a whole membrane. Nanosized UiO-66-NH_2 was polymerized induced by UV light with the aid of methacrylic anhydride and butyl methacrylate after the formation of UiO-66-NH_2 (Fig. 19), which strengthen the connection between polymer chains and MOF particles. According to the report, the strong combination between the MOF and polymer chains leads to fewer cracks in the membrane and high separation capacity, but the synthesis of nanocrystals of MOFs could be difficult, indicative of the

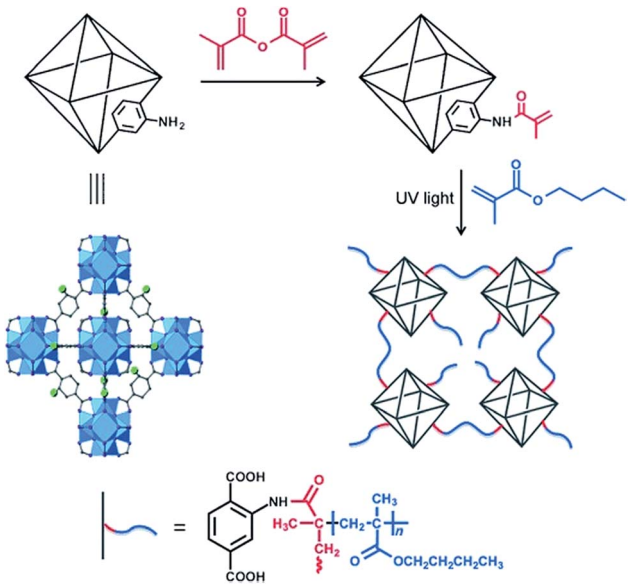

Fig. 19 Post-synthetic polymerization of UiO-66-NH_2 with the aid of methacrylic anhydride and butyl methacrylate under the irradiation of UV light.[149] Copyright © 2015 John Wiley & Sons, Inc.

extremely complex procedures of the postsynthetic polymerization method.

3.1.6 Pressure-assisted preparation method. As a way to obtain a strong combination between MOF membranes and substrates, the pressure-assisted preparation method has been developed. Generally, one side of the matrix is immersed into the precursor solution, and pressure is applied on the other side. The solution could penetrate through the matrix under the action of pressure difference and a homogeneous membrane could be obtained. Peng *et al.* prepared a HKUST-1 membrane based on polyvinylidenefluoride (PVDF) which is precoated with copper hydroxide nanostrands (CHN). The process of the preparation can be summarized as in Fig. 20. One end of the PVDF hollow fiber was sealed with suction filtration in order to achieve the precoating. Then the HKUST-1 membranes were prepared by immersing the modified PVDF hollow fibre into an ethanol/water solution of H_3BTC at room temperature under an external pressure of 90 kPa which was applied by using a vacuum pump.[150] This strategy leads to dense membranes and a strong combination between MOF membranes and substrates. Obviously, matrices with high permeability are also required in this method.

3.1.7 Spray method. The MOF powder prepared by solvothermal methods is usually difficult to process. It is still needed to enable the fabrication of large-area and well-performing MOF membranes. In a previous study,[151] a spray method was developed to obtain large-area MOF membranes and control the thickness of MOF membranes. Precursor solutions are sprayed with moveable nozzles alternatively on the substrate. The spray nozzles of different precursor solutions are moved in front of the substrate so as to enable the even distribution of the solutions, which leads to large-area membranes. For example, in order to obtain a HKUST-1 membrane, ethanolic solutions of trimesic acid and copper(II) acetate are both used and an energy dispersive X-ray spectrometer (EDX) exhibits the homogeneity of the HKUST-1 membrane on the support (Fig. 21). In this strategy, the maximum size of the membrane is only decided by the traverse paths of the spray

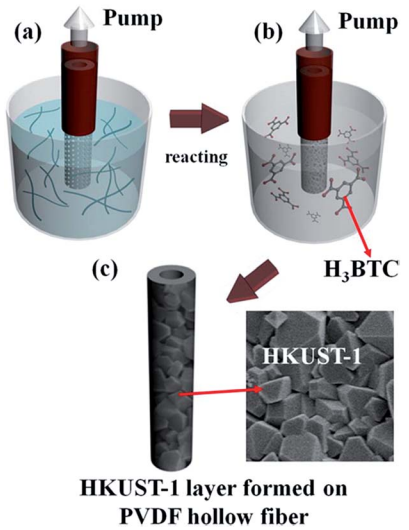

Fig. 20 Preparation of a HKUST-1 membrane based on PVDF hollow fibers precoated with CHN.[150] Copyright 2014, American Chemical Society.

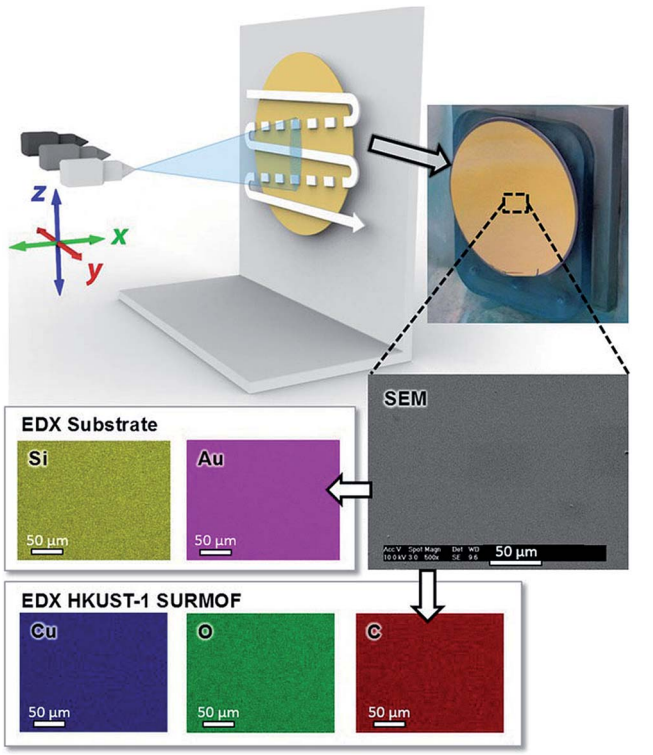

Fig. 21 Synthesis of HKUST-1 using the spray method and the EDX images of the MOF membrane.[151] Copyright © 2017 John Wiley & Sons, Inc.

nozzles. Not only the size but also the thickness of the membranes is controllable.

3.1.8 Ligand-induced permselectivation method. Recently, a ligand-induced permselectivation (LIPS) approach was developed by Tsapatsis *et al.*, which was used to prepare a ZIF-8 membrane.[152] This method is mainly based on atomic layer deposition, which will be discussed later. Briefly, ZnO was deposited on a porous Al_2O_3 matrix through a reaction between diethylzincs and hydroxy groups in an Al_2O_3 matrix, and the pores of the matrix were blocked, which exhibits a low propylene flux; then the composite was treated with mIm ligand-vapor to form ZIF-8, which allows the entrance of propylene. This LIPS method endows membranes with excellent separation capacity.

3.2 Applications of MOF membranes

As defined earlier, MOF membranes mainly refer to 2D-architectured MOFs with separation or separation-based functions. Therefore, they are frequently applied to some special fields, which are going to be discussed in detail.

3.2.1 Separation. The efficient separation of gas mixtures is of great societal and industrial value. Membrane technology has been widely used in purification and separation processes due to its low energy consumption, good safety, good environmental compatibility and short operating time since the late 1960s.[153,154] Membrane-based separations have obvious advantages in large-scale applications when compared with other strategies.[155–157] As for MOFs, their selective adsorption,[158,159] high surface areas and uniform pore sizes[41] demonstrate that they have great potential in separation. Compared with zeolites and polymers, moderate compliance of pores imparts to MOFs great separation performance.[160] MOFs are structurally flexible, which is beneficial for applications where elasticity is needed, such as adsorption-based separation. One can tune the guest adsorption by changing the structure of flexible MOFs.[161] Due to the advantages of both the membrane and MOF in separation technology, MOF membranes are ideal candidates for separation. Besides, the high porosity, large surface area, high energy efficiency, easy operation, low cost and recyclability enable MOF membranes to be applied in gas separation.[8,41,162] Hence, MOF membranes are suitable for separation. In fact, MOF membranes have been developed as a unique medium for gas separation over the past decade.[163] Building blocks in the nanoparticulate form and/or with large aspect ratios are needed to obtain formation of membranes and improved separation performance.[164] There have been some reviews on the separation properties of MOF membranes.[113,143,160,165–172] However, some problems arise when MOF membranes work as molecular sieving membranes. Generally, it is recommended that MOFs are deposited on the surface of inorganic substrates (*e.g.* TiO_2) when applying them as molecular sieving membranes, but the accomplishment of this strategy is limited by the brittleness of the inorganic substrates and high cost. And the lack of active sites on the surface of inorganic substrates also makes the deposition harder. The modification of inorganic substrates can be developed as a good way to solve these problems.[173] And apart from MOF membranes, monolayer films based on 2D MOFs have also been expected to act as an important source of nanosheets for separation,[174] which will soon be discussed later.

Generally, the assessment of the separation properties is based on selectivity and separation factors. The definition of gas selectivity (α) for a binary gas mixture can be summarized by eqn (1):

$$\alpha = \frac{y_i x_j}{y_j x_i} \quad (1)$$

in which y_i and y_j refer to the mole fraction of species i and j in the permeate stream while x_i and x_j are the mole fraction of species i and j in the feed stream, respectively.[168,175]

ZIF-8 is a great candidate for gas separation due to its self-assembly.[176] To evaluate the adsorption performance of ZIF-8 nanoparticles on different alcohols, polymethylphenylsiloxane (PMPS) was used as a polymer substrate to prepare organophilic pervaporation membranes. The membranes were prepared in the interior of a cathedral capillary *via* a solution-blending dip-coating method, and denoted as ZIF-8-PMPS membranes (Fig. 22a). The pervaporation recovery of isobutanol on the ZIF-8-PMPS membrane was tested and the separation factor is between 34.9 and 40.1. The permeability and separation factors of the ZIF-8-PMPS membranes are superior to those of most OPV membranes which have already been reported (Fig. 22b). In addition, the ZIF-8-PMPS membrane can also recover other alcohols from water (Fig. 22c), and the recovery rate is considerable.[161] Additionally, the ZIF-8-PMPS membrane can also be loaded on a hierarchically ordered stainless-steel-mesh (HOSSM), which exhibits considerable separation properties

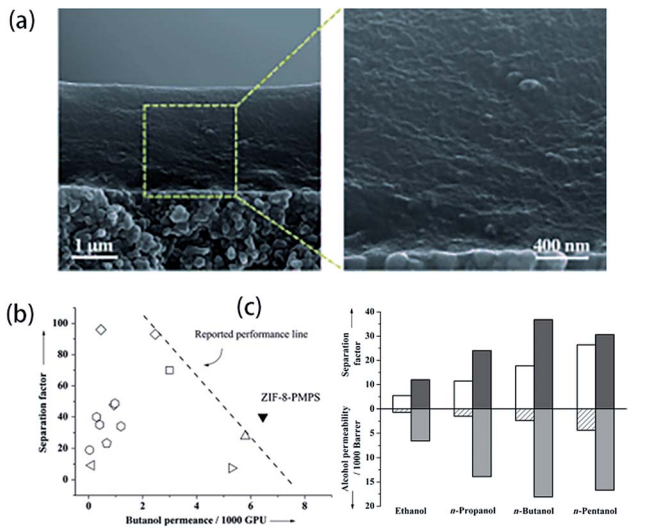

Fig. 22 (a) SEM images of the ZIF-8-PMPS membrane from the cross view; (b) the H_2O and butanol separation factor *versus* permeance for different membranes and 1 GPU refers to 1×10^{-6} cm^3 (STP) cm^{-2} s^{-1} cm Hg^{-1}; (c) alcohol permeability as well as separation factor of PMPS membranes, which are shown as line filled and open columns, and ZIF-8-PMPS membranes, which are shown as light gray and gray columns, for different alcohols in aqueous solution, and 1 barrer refers to 1×10^{-10} cm^3 (STP) cm cm^{-2} s^{-1} cm Hg^{-1}.[161] Copyright © 2011 John Wiley & Sons, Inc.

towards furfural/water.[177] Similarly, ZIF-8 membranes have been prepared in the interior of a cathedral capillary and 3-aminopropyltriethoxysilane was used as the substrate.[178]

Global warming and the energy crisis have become very important concerns.[34,179] CO_2 separation from a flue gas attracts much attention of researchers. Currently, the separation of CO_2 from a mixed gas is accomplished mainly by sorption or cryogenic methods; however, the application of both of these methods is limited by their high cost and low efficiency. Thus, it is crucial to find an efficient environmental-friendly method to realize the separation of CO_2.[180] Membrane-based separation properties are usually limited by the trade-off between selectivity and permeability.[181,182] The combination between the molecular sieving and the adsorption properties of MOFs and the processing properties of polymers could lead to gas selective membranes.[183] MOFs and polymers are usually combined to form mixed matrix membranes (MMMs), which could improve the separation properties of MOF membranes. Urban *et al.* reported a hybrid membrane with dual transport pathways, which is based on UiO-66-NH_2 as well as PSF. Gas molecules can permeate the membrane through both UiO-66-NH_2 and PSF. This hybrid membrane isn't affected by the trade-off. In their study, UiO-66-NH_2 was dispersed in PSF solution and sonicated. The solution was then dropped on the surface of a substrate and evaporated, and then the hybrid membrane was formed. The permeability and selectivity of CO_2, CH_4, and N_2 in different mass fractions of UiO-66-NH_2 are provided (Fig. 23). For convenience, we name these membranes which contains different contents of MOF after the mass fraction of UiO-66-NH_2. According to the result, at 40 wt%, the CO_2 permeability is 8.1 times higher than that of pure PSF, which is 46 barrer. This membrane is denoted as UiO-66-NH_2/PSF (40 wt%). The permeabilities of all hybrid membranes are apparently higher than those of pure PSF membranes (Fig. 23a). And as shown in Fig. 23b, there is little relationship between the selectivity of the hybrid membrane and the mass fraction of UiO-66-NH_2.[182] In addition, COFs have also been used in the separation field. COFs are crystalline polymers which could be obtained from various organic building blocks and have porous structures with a high surface area.[184–187] Gao *et al.* successfully loaded different doses of Schiff based COFs (SNW-1) on PSF, and tested their separation capabilities. As a result, the separation factors reach the maximum when the content of SNW-1 is 12 wt%, and are 40 and 34 for CO_2/N_2 and CO_2/CH_4, respectively, and the membranes is denoted as SNW-1/PSF (12 wt%).[180] Similarly, Mustafa *et al.* modified ZIF-8 with amino and dispersed it in a PSF matrix to form a dual transport pathway,[188] and Zornoza *et al.* dispersed NH_2-MIL-53(Al) in a PSF membrane to prepare NH_2-MIL-53(Al)/PSF and obtained a high CO_2/CH_4 separation selectivity.[189] Besides, polyamide can also work as a substrate when MOFs work as fillers.[190] In fact, the interactive thermal effects on PSF-based MOF membranes have been studied.[191] Especially, Kertik *et al.* dispersed amorphous ZIF-8 in polyimide (PI) *via* the *in situ* method and obtained hybrid membranes with different mass percents of ZIF-8 after treated at different temperatures. According to the separation experiment, the hybrid membrane with 30 wt% ZIF-8 (ZIF-8/PI (30 wt%)) which is treated at 350 °C exhibits the highest CO_2/CH_4 selectivity, which is 162. And ZIF-8/PI (40 wt%) which is treated at 160 °C exhibits the highest CO_2 permeability of 57 barrer.[192] A MOF $[Cd_2L(H_2O)]_2 \cdot 5H_2O$ (Cd-6F)[193,194] was combined with 4,4′-(hexafluoroisopropylidene) diphthalic anhydride-4,4′-oxydianiline (6FDA-ODA) polyimide to obtain a MMM, which exhibits an enhanced separation properties towards CO_2/N_2 and CO_2/CH_4.[195] Lots of similar studies that use polymer materials as the substrates have also been reported.[175,196–201] Some derivatives of PSF have also been used as substrates.[202]

In contrast, a polymer membrane based on a MOF was developed, which exhibits optimal CO_2/N_2 separation properties which have been reported.[203] A raw MOF/anodisc (RMA) was developed by modifying the amino group in NH_2-MIL-53 with α-bromoisobutyryl bromide and immersing this MOF membrane in solutions of polyethylene glycol dimethacrylates (PEGDMA) in different concentrations. The PMA membranes obtained from different concentrates of PEGDMA are denoted as PMA-A, -B and -C (PMA-A < PMA-B < PMA-C). As a result, PMA-C has the highest selectivity for CO_2/N_2 separation among the three membranes but without a high CO_2 permeance. PMA-B was expected to have the best CO_2/N_2 separation properties, with a selectivity of 34 and a CO_2 permeance of 3000 GPU.

Generally, the ionic liquid decoration strategy could serve as an efficacious method to fill the interfacial pores in MMMs.[204] Ionic liquids@MOF membranes also show separation capacities for gas mixtures such as CO_2/N_2. The selectivity of CO_2/N_2 and CO_2 permeability in the composite BMI-SCN@IRMOF-1 (BMI^+ = 1-butyl-3-methylimidazolium, SCN^- = thiocyanate) membrane and [BMIM][PF_6]@IRMOF-1 ([BMIM][PF_6] = 1-*n*-butyl-3-methylimidazolium hexafluorophosphate) membrane have been studied respectively.[205,206] This research indicates that ionic liquids@MOF membranes also exhibit separation capacity.[207]

It is difficult to rely on experiments to test all the MOFs one by one to evaluate their gas separation performance.[208] Sumer *et al.* evaluated the CH_4/N_2 separation capacities of 102 MOFs with the aid of Grand Canonical Monte Carlo (GCMC). According to their conclusion, the MOFs that have these properties always exhibit better separation capacities for CH_4/N_2,

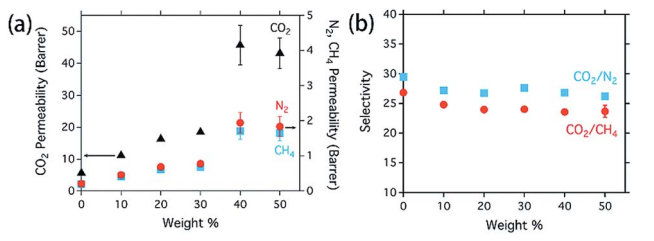

Fig. 23 (a) Permeabilities of CO_2 (shown as triangles), N_2 (shown as squares), and CH_4 (shown as circles) at 35 °C and 3 bar of hybrid membranes in various mass fractions of UiO-66-NH_2. Error bars in the figure refer to single standard deviation; (b) ideal hybrid gases of CO_2/N_2 (shown as squares) and CO_2/CH_4 (shown as circles) selectivity at 35 °C and 3 bar of hybrid membranes in various mass fractions of UiO-66-NH_2. Error bars in the figure refer to single standard deviation[182] Copyright 2016, Royal Society of Chemistry.

which are (1) pore limiting diameters ranging from 2.4 to 3.7 Å, (2) largest cavity diameters ranging from 4.6 to 5.4 Å, (3) porosities less than 0.5 and (4) surface areas less than 2000 $m^2 g^{-1}$.[209]

Besides the deposition of MOF membranes on substrates, it is also feasible to deposit MOF nanoparticles in the pores of porous substrates in order to improve the permeability and rejection properties of composite membranes.[210,211]

Interestingly, Knebel *et al.* found that an external electric field can stiffen the ZIF-8 lattice through polarization and reduces the molecular transport and improves its molecular sieving capability.[212] Hara *et al.* synthesized a HKUST-1 membrane within the pores of an α-alumina substrate, which possesses an advanced H_2/CH_4 selectivity.[213]

Jiang *et al.* reported a computational method to screen the best MOFs for the separation of N_2 as well as CO_2 from CH_4 from 137 953 MOFs *via* single-step membrane separation without adsorption. Four steps are consisted in the strategy (Fig. 24a), which are (1) the calculation of the pore limiting diameters (PLDs) to select 17 257 MOFs with a diameter of 3–4 Å, (2) the estimation of Henry's constants and diffusivities of CH_4, N_2, and CO_2 in the 17 257 MOFs at 298 K and the quantitative relationships *versus* the PLD are found, (3) the pre-screening of 24 MOFs based on permselectivity and (4) the simulation of the permeation, diffusion, and adsorption of $CH_4/N_2/CO_2$ in the 24 MOFs at a temperature of 298 K and the pressure of 10 bar. Finally, the 5 best MOFs for the separation of N_2 as well as CO_2 from CH_4 were found. This computational study reveals that the percentage of pore size distribution and the PLD are two key factors which have a high effect on diffusion and permeation. According to a report, there is a positive correlation between P^o and PLD, volumetric surface area (VSA), and porosity (φ), which is shown in Fig. 24b–d.[214]

Differently, the separation capacities of MOF membranes are sometimes related to the orientation of crystals. The oriented growth of MOFs is essential for separation application because the orientation of MOF crystals dictates the penetration directions of target gases.[215] The selectivities of HKUST-1 membranes towards CO_2/SF_6 are 1.9 and 13.1 when the preferred orientations are [001] and [111], which is related to the kinetic diameters of gas molecules.[216] According to an earlier report, the orientation of crystals could be confirmed by X-rays,[215] which could be helpful for the oriented growth of MOF thin films and membranes.

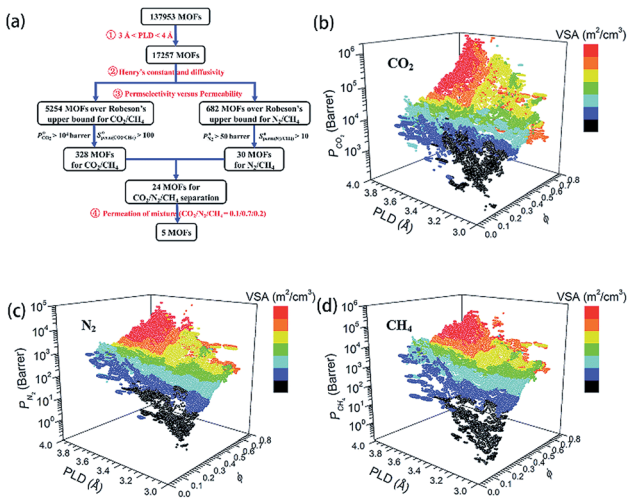

Fig. 24 (a) The scheme of the screening strategy. (b) The relationship between permeability *P versus* VSA, φ, and PLD for N_2, CO_2, and CH_4.[214] Copyright 2016, Royal Society of Chemistry.

Additionally, the anisotropic thermal expansion of MOF membranes and thin films should be considered to improve the separation properties. MOF membranes which exhibit pronounced stability in heating–cooling cycles could be applied to membrane separation. The anisotropic thermal expansion of a HKUST-1 SURMOF membrane based on a gold substrate was studied. The HKUST-1 SURMOF membrane exhibited apparent stability in heating–cooling cycles despite the mismatch of anisotropic thermal expansion at the interface. Thus, the HKUST-1 SURMOF membrane could be used for membrane separation at high temperatures.[217] More efforts should be made to control the thermal expansion behaviors of MOF materials to obtain enhanced separation properties.

In general, according to these reports, we can draw the conclusion that the separation properties of MOF-based membranes can be improved by these following strategies: (1) applying an appropriate external electric field; (2) combining a MOF membrane and substrate which both have good separation properties to achieve a dual transport pathway; (3) depositing MOF nanoparticles on porous substrates to improve the hole structure; (4) choosing an optimal orientation; (5) combining two materials with different selectivity and flux to obtain a membrane with better separation capacity, such as the combination between polymers with easy processability and MOFs with superior separation properties.[218,219] Altogether, the separation capabilities of different MOF-based membranes are concluded as in Table 1.

Various substrates are suitable for the deposition of MOF films and membranes, such as titania, alumina, silica, graphite, and nylon.[220] Especially, some types of matrices which are beneficial for the improvement of separation capacity are summarized as follows: (1) α-Al_2O_3; (2) polymer substrates, such as PSF and polyoxazoline (POZ);[201] (3) organosilica;[221] (4) foam substrates, *e.g.* Ni-foam substrates.[222]

Apart from gas separation, nanoparticle filtration could also be achieved by using 2D MOFs. A type of 2D MOF in the form of powder or monolayer films was prepared using tri(β-diketone) and Cu^{2+} ions. According to the report, it could be used in the size-selective filtration of Au nanoparticles with a cutoff of about 2.4 nm.[223]

3.2.2 Water treatment. Previously, we have reviewed the catalytic properties of MOFs and COFs, and a wastewater treatment based on catalysis is involved in the earlier review.[34] Herein, we are going to introduce some reports about wastewater treatment based on adsorption and separation. A polytetrafluoroethylene (PTFE) microfiltration membrane was modified with ZIF-8 and applied for the removal of micropollutants from water, which is denoted as ZIF-8-PTFE. The ZIF-8-PTFE membrane was prepared *via* a solvent evaporation

Table 1 Comparison between different MOF-based membranes and thin films

Membrane	Substrate	Mixture	Temp. (°C)	Separation factor	Permeance	Ref.
SNW-1/PSF (12 wt%)	PSF	CO_2/N_2	25	40	25.04 barrer (CO_2)	Gao *et al.*[180]
SNW-1/PSF (12 wt%)	PSF	CO_2/CH_4	25	34	25.04 barrer (CO_2)	Gao *et al.*[180]
NH_2-MIL-53(Al)/PSF (25 wt%)	PSF	CO_2/CH_4	35	46	6 barrer (CO_2)	Zornoza *et al.*[189]
ZIF-8/PI (30 wt%)	PI	CO_2/CH_4	35	162	4.5 barrer (CO_2)	Kertik *et al.*[192]
ZIF-8/PI (40 wt%)	PI	CO_2/CH_4	35	20	57 barrer (CO_2)	Kertik *et al.*[192]
HKUST-1	Matrimid®	CO_2/CH_4	35	~26	17 GPU (CO_2)	Vankelecom *et al.*[224]
ZIF-8	Matrimid®	CO_2/CH_4	35	~23	22 GPU (CO_2)	Vankelecom *et al.*[224]
MIL-53(Al)	Matrimid®	CO_2/CH_4	35	~27	19 GPU (CO_2)	Vankelecom *et al.*[224]
ZIF-90	TOCN	CO_2/CH_4	RT	123	2.97×10^3 GPU (CO_2)	Kitaoka *et al.*[225]
Cd-6F	6FDA-ODA	CO_2/CH_4	25	44.8	37.8 barrer (CO_2)	Ge *et al.*[195]
NH_2-MIL-101(Al)	CNT/PI	CO_2/CH_4	25	25.4	1037 barrer (CO_2)	Ge *et al.*[226]
IRMOF-1	Matrimid	CO_2/CH_4	35	40.5	~20 barrer (CO_2)	Sholl *et al.*[227]
ZIF-8	α-Al_2O_3	C_3H_6/C_3H_8	RT	~50	~100 barrer (C_3H_6)	Jeong *et al.*[140]
ZIF-8 (LIPS)	Al_2O_3	C_3H_6/C_3H_8	RT	~100	$>10^{-8}$ mol Pa^{-1} m^{-2} s^{-1} (C_3H_6)	Tsapatsis[152]
HKUST-1	α-Alumina substrate	H_2/CH_4	25	153	2.45×10^{-9} mol m^{-2} s^{-1} Pa^{-1} (CO_2)	Hara *et al.*[213]
NH_2-MIL-53(Al)	Macro-porous glass frit support	H_2/CH_4	15	27.3	1.517×10^{-6} mol m^{-2} s^{-1} Pa^{-1} (H_2)	Zhu *et al.*[228]
ZIF-8	P84 hollow fibers	H_2/CH_4	35	103	3.5×10^{-8} mol m^{-2} s^{-1} Pa^{-1} (H_2)	Coronas *et al.*[229]
ZIF-93	P84 hollow fibers	H_2/CH_4	35	101	1.0×10^{-8} mol m^{-2} s^{-1} Pa^{-1} (H_2)	Coronas *et al.*[229]
ZIF-8/organosilica	Tubular α-Al_2O_3	H_2/CH_4	RT	35.0	1.06×10^{-6} mol m^{-2} s^{-1} Pa^{-1} (H_2)	Kong *et al.*[221]
IRMOF-1	Matrimid	H_2/CH_4	35	112	~20 barrer (CO_2)	Sholl *et al.*[227]
HKUST-1@PI	PI	CO_2/CH_4	25	88.2	2.78 barrer (CO_2)	Rodenas *et al.*[230]
$Zn_2(bim)_4$	—	H_2/CO_2	80–200	53–291	760–3760 GPU (H_2)	Peng *et al.*[174]
ZIF-78	Porous ZnO	H_2/CO_2	25	11.0	7.2×10^3 barrer (H_2)	Jin *et al.*[231]
ZIF-8	PMPS@HOSSM	Furfural/water	80	53.3	12.2×10^4 barrer (furfural)	Liu *et al.*[177]
HKUST-1	P84	Ethylene/ethane	150	7.1	1.7×10^{-17} mol m m^{-2} s^{-1} Pa^{-1} (ethylene)	Nijmeijer *et al.*[200,232]
Cu-BTC-S2 (40 wt%)	PPO	CO_2/N_2	30	~26	~110 barrer (CO_2)	Zhu *et al.*[133]
NH_2-UiO-66-ABA	Matrimid 9725	CO_2/CH_4	35	47.7	37.9 (CO_2)	Vankelecom *et al.*[137]
ZIF-8	Tubular α-Al_2O_3	CO_2/CH_4	65	7.0	2.42×10^{-6} mol m^{-2} s^{-1} Pa^{-1} (CH_4)	Carreon *et al.*[233]
PMA-A	Porous anodisc substrate	CO_2/N_2	35	~1.2	~15 000 GPU (CO_2)	Webley *et al.*[203]
PMB-B	Porous anodisc substrate	CO_2/N_2	35	34 ± 3	>3000 GPU (CO_2)	Webley *et al.*[203]
PMB-C	Porous anodisc substrate	CO_2/N_2	35	37 ± 2	310 ± 30 GPU (CO_2)	Webley *et al.*[203]
ZIF-69	α-Alumina substrate	CO_2/N_2	25	2.2	$23.6 \pm 1.5 \times 10^{-9}$ mol m^{-2} s^{-1} Pa^{-1} (CO_2)	Lai *et al.*[234]
Cd-6F	6FDA-ODA	CO_2/N_2	25	35.1	37.8 barrer (CO_2)	Ge *et al.*[195]
ZIF-7	Asymmetric alumina discs	H_2/N_2	220	18.0	~4.5×10^{-8} mol m^{-2} s^{-1} Pa^{-1} (H_2)	Li *et al.*[235]
HKUST-1 (out)	PBI-BuI-HF	He/N_2	35	12	1.31 GPU (He)	Banerjee *et al.*[144]
HKUST-1 (in)	PBI-BuI-HF	He/N_2	35	8	0.89 GPU (He)	
HKUST-1 (out)	PBI-BuI-HF	He/C_3H_8	35	17	1.31 GPU (He)	
HKUST-1 (in)	PBI-BuI-HF	He/C_3H_8	35	8.7	0.89 GPU (He)	
ZIF-8 (out)	PBI-BuI-HF	He/N_2	35	4.2	1.80 GPU (He)	
ZIF-8 (in)	PBI-BuI-HF	He/N_2	35	3.7	2 GPU (He)	
ZIF-8 (out)	PBI-BuI-HF	He/C_3H_8	35	4.6	1.80 GPU (He)	
ZIF-8 (in)	PBI-BuI-HF	He/C_3H_8	35	8	2 GPU (He)	

strategy. The removal is based on adsorption. Progesterone was used as the model pollutant in order to test the filtration performance of the membrane. According to the result, the removal of progesterone reaches nearly 100% in about 24 hours, indicating the considerable filtration performance of the ZIF-8-PTFE membrane.[236] MOF-polylactic acid (PLA) membranes were developed *via* an *in situ* growth method. A Cu-MOF was chosen in this study, and the MOF membranes was based on the PLA substrate obtained by 3D printing. The Cu-MOFs/PLA membranes can absorb malachite green (MG) in waste water, and researchers observe a >90% removal efficiency in adsorbing MG for 10 minutes. A number of adsorption/desorption cycles were performed to examine the recyclability of Cu-MOFs/PLA membranes. The membrane exhibits a removal efficiency of 80% for MG after three cycles, while a removal efficiency of 60% after five cycles. The Cu-MOFs/PLA membranes could also be a potential candidate for wastewater treatment because of their adsorption capacity for MG.[237]

Membrane-based capacitive deionization (MCDI) attracts people's attention. As a potential water desalination method, it is expected that it can help solve the water shortage problem. Ding *et al.* synthesized bimetallic metal–organic frameworks (BMOFs) with different Co and Zn molar ratios based on ZIF-67 and ZIF-8 and obtained derivatized carbides of these BMOFs. These carbides can remove NaCl from the solution. The device model is shown in Fig. 25, which is used to test the desalting capacity. The conductivity of the solution reflects the amount of residual NaCl. The desalting capacity of the porous carbon obtained when the Zn : Co ratio is 3 : 1 was 45.62 mg g^{-1} in a 1.4 V environment.[238] This study can be used for seawater desalination. Therefore, the most common methods of wastewater treatment are adsorption, catalysis and filtration. In view of these aspects, more efficient devices could be designed and constructed for wastewater treatment.

3.2.3 Battery systems and fuel cells. Energy consumption will increase steeply by 56% from 2010 to 2040. In order to solve this problem, several new energy technologies have been proposed, including new battery technology.[239] The tunability of the structure and the function of MOFs endow them with excellent functions in mass transport in the battery system: (1) absorbing specific ions or molecules to limit them in a differential region; (2) preventing ions and molecules from passing across it except for some specific ions or molecules, according to the review published by Zhou *et al.*[240] The poor physical connection between the solid-state battery and the electrodes results in large interfacial resistance.[241–243] Hence, based on the definition of MOF membranes we proposed, it is MOF membranes that are used in battery systems.

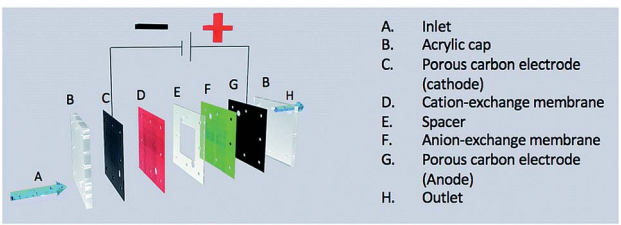

Fig. 25 The sketch of the MCDI testing cell.[238] Copyright 2017, Royal Society of Chemistry.

However, in fact, MOF membranes usually exhibit poor electroconductivity, indicating that the MOFs used in battery systems are frequently derived (*i.e.* carbonized) in order to improve their conductivity.[244] Lithium-ion batteries which exhibit high energy density and low self-discharge without memory effects are always regarded as the energy sources for portable electronic equipment,[245–247] electric cars and smart grid systems,[248–250] according to previous reports and reviews. MOF-derived hollow and porous carbon nanostructures may store more lithium due to their large surface areas, reduced Li^+ diffusion distance and the mechanical stress buffering caused by the void space.[251] For instance, Lou *et al.* prepared multi-shelled Co_3O_4@$Co_3V_2O_8$ nanoboxes from ZIF-67, which were used in lithium-ion batteries as electrode materials in the study. Besides, ZIF-67 derived symmetric Co_3O_4 hollow dodecahedra have been reported, which has an enhanced lithium storage capability.[252] Similarly, $Mn_{1.8}Fe_{1.2}O_4$ nanocubes[253] and ZnO/$ZnCo_2O_4$/C hybrids[254] derived from MOFs were obtained, which also improve the performances of lithium ion batteries. Apart from lithium-ion batteries, derivatives of MOFs could also be used in sodium-ion batteries. Various types of MOFs are employed to obtain high electrical performing composites, such as Co_9S_8/ZnS,[255] Co_3O_4/ZnO,[256] Nb_2O_5/C,[257] $CoSe_2$/ZnSe[258] and MoS_2/C hybrids,[259] which have high sodium storage capacity. We expect that, more efficient lithium- and sodium-ion battery materials will be developed from MOF-based membranes and thin films.

4. MOF films

According to our aforementioned definition, MOF thin films mainly refer to the ones without separation-based performances, which makes them different from MOF membranes. Therefore, they may not exhibit 2D-type performances. However, it is still meaningful and useful to continue the study of MOF thin films. We could design and synthesize MOFs from the perspective of films. We could obtain MOFs *via* a film-forming method, and thus optimize the structural integrity by regarding the materials as thin films rather than just bulks. In other words, although MOF thin films may not show 2D-type performances, their study provides some new ideas for the design and synthesis of MOFs. The first MOF film is synthesized *via* the solvothermal method by Hermes *et al.*[260] An excellent review about MOF films has been published earlier.[261] Many excellent reviews have summarized some classical synthetic methods of MOF films, including *in situ* growth, secondary growth, the liquid-phase epitaxy (LPE) method and so on. Herein, we summarize some new research concerning the synthesis of MOF thin films and some new synthetic strategies.

4.1 Synthetic methods of MOF films

4.1.1 Solvent method. Various synthetic methods have been proposed to improve the performances of MOF films or endow them with special functions. Guo *et al.* have prepared

a NbO-type MOF denoted as $Cu_2(EBTC)(H_2O)_2 \cdot [G]$ (EBTC refers to 1,1′-ethynebenzene-3,3′,5,5′-tetracarboxylate; G refers to different ligands), which is based on paddle-wheel-type dinuclear Cu_2 SBUs and the $EBTC^{4-}$ linker. Interestingly, different MOFs can be obtained by filling the pores with different ligands. Provided that DMSO, DMF and H_2O occupy the pores, the MOF is denoted as **1**; the MOF is named **2** when H_2O and CH_3OH fill the pores. **1** and **2** can be synthesized *via* a solvothermal method on Al_2O_3, and the composites are denoted as **1**/Al_2O_3 and **2**/Al_2O_3, respectively. They exhibit thermochromism properties. Both of them have the same trend with temperature change. Their color deepens when temperature increases (Fig. 26). Most interestingly, these changes are reversible. According to the authors, this reversible change is due to lattice expansion, which leads to the change of coordination situation. Then the color of the film is changed.[262]

A general method which can encapsulate various functional components in MOF films *via* a metal-hydroxide-nanostrand-assisted method based on solvent has been developed.[263] Five negatively charged functional species were encapsulated into a HKUST-1 film based on CHN, including $[AuCl_4]^-$, Au nanoparticles, ferritin and glucose oxidase, polystyrene spheres and single-walled carbon nanotubes (CNTs). The negatively charged functional species were incorporated into CHN thin films by mixing the component dispersion,[264] and HKUST-1 was synthesized based on the modified CHN (Fig. 27). From this encapsulated strategy, some bio-electrochemical, synergistic and size-selective catalytic, conductive and flexible materials could be constructed *via* encapsulating different species into diverse MOFs.[263]

From the traditional solvothermal method, a microcontact click printing strategy was developed. Silicon wafers could be patterned with carboxylic acid functional groups by employing copper-catalyzed alkyne–azide cycloaddition. A MOF-5 thin film could be subsequently prepared (Fig. 28a). Generally, silicon wafers which have been functionalized with alkylazides are subjected to printing with pentynoic acid and copper to form rows of pentynoic acid and unreacted azide. Then the wafers were dealt with the DEF solution of $Zn(NO_3)_2 \cdot 6H_2O$ and terephthalic acid to form a MOF-5 thin film. Finally, the large

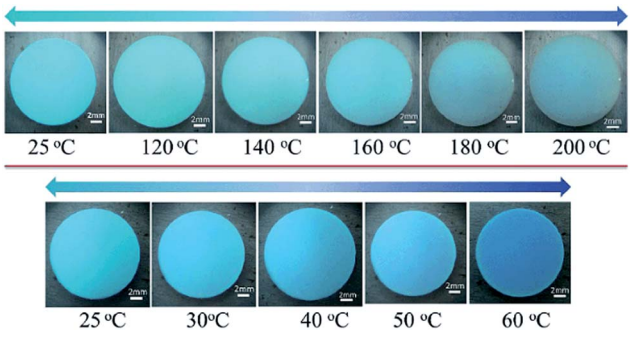

Fig. 26 The upper and lower columns of the pictures indicate the changes in the color of the **1**/Al_2O_3 film and **2**/Al_2O_3 film, respectively, as the temperature increases.[262] Copyright 2014, Royal Society of Chemistry.

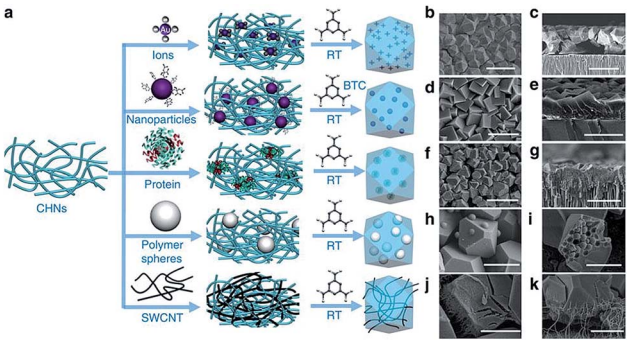

Fig. 27 Illustration of the encapsulation process and SEM images of the thin films.[263] Copyright © 2014, Springer Nature.

crystals are removed mechanically. The SEM and AFM images of the MOF-5 thin film are shown in Fig. 29b and c, respectively, which show the apparent boundaries between the rows of MOF-5 and the rows of unreacted azide.[265]

Besides, a ZIF-8 film was grown on a copper-based substrate *via* secondary growth with the assistance of acetate, and according to the report, the addition of acetate might lead to bigger crystals, which further results in oriented crystals in planes {200} and {110}. Hence, the employment of acetate could

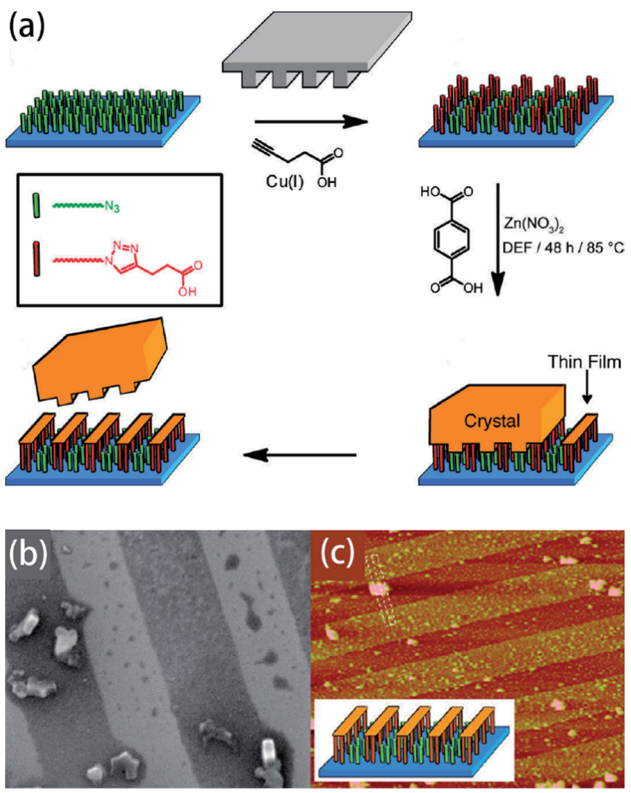

Fig. 28 (a) The schematic illustration of the microcontact click printing synthesis of the MOF-5 film. (b) The SEM image of the as-prepared film, in which the dark region refers to the MOF-5 film. (c) The AFM image of the as-prepared film, in which the dark region refers to the unreacted azide surfaces.[265] Copyright 2011, American Chemical Society.

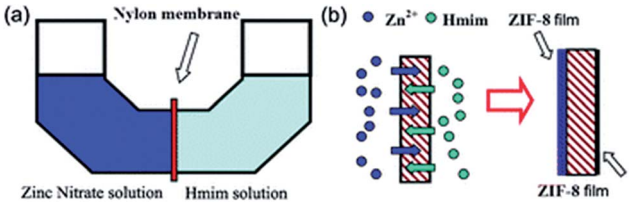

Fig. 29 (a) Diffusion device for the preparation of ZIF-8 films; (b) the diagram of the ZIF-8 films on the both sides of the nylon substrate *via* the contra-diffusion method of two solutes (Hmim and Zn^{2+}) through the pores of the nylon substrate.[142] Copyright 2011, Royal Society of Chemistry.

give rise to MOF thin films with oriented crystals, which have excellent mechanical and thermal stability.[266]

The aforementioned concept we propose in this review demonstrates that there do not exist many differences between MOF membranes and thin films at the level of chemical essence. Since the general strategy and properties of the solvent method have been discussed in Section 3.1.1, in view of the simplification of this review article, we do not explore it in detail here.

4.1.2 Electrochemical deposition. Electrochemical deposition has been used to construct MOF films. Typically, as for cathodic electrodeposition, a two-electrode cell is frequently employed for the electrochemical deposition. A graphite rod usually serves as the anode while Fluorine-doped Tin Oxide (FTO) conductive glass works as the cathode. A solution of nitrate and ligand act as the electrolyte solution. Cathodic generation of hydroxyl ions could lead to the deprotonation of the ligand. Metal ions move to the cathode and further cause the growth of MOFs on the FTO conductive glass.[267] Actually, some excellent reviews have summarized the electrochemical deposition of MOFs.[92,121,268] Kaur *et al.* reported a kind of graphene–MOF composite based on graphene and Eu-MOF. This composite film can be prepared *via* electrochemical deposition. The Eu-MOF can be synthesized *via* mixing 1,3,5-tris(4-carboxyphenyl)benzene (H_3BTB) and $Eu(NO_3)_3 \cdot 5H_2O$. Then an aqueous suspension of graphene and a DEF dispersion of Eu-MOF are mixed, following by putting in an electrochemical cell, in which TiO_2/FTO works as the electrode. A graphene–MOF composite film is deposited on TiO_2/FTO.[269] Liu *et al.* obtained a $[\{[Eu(HBPTC)(H_2O)_2] \cdot 2DMF\}_n]$ (BPTC refers to benzophenone-3,3′,4,4′- tetracarboxylate) film, which is denoted as Eu-HBPTC *via* this method, and the film can be applied to a photoluminescent device and chemical sensor, which will be demonstrated later.[270] Besides, a patterned luminescent MOF thin film was grown *via* an electrochemically assisted microwave deposition strategy, which could have potential for anti-counterfeiting barcode applications.[271] The electrodeposition method could give rise to MOF thin films with controllable thickness. However, metal ions with high inertness might separate out on the cathode and the ligands might be oxidized.

4.1.3 Contra-diffusion method. As mentioned earlier, a ZIF-8 film can be synthesized *via* a contra-diffusion method, which is based on a nylon substrate. Just as Fig. 29 shows, the two solutions diffuse from opposite sides of the nylon membrane in opposite directions and ZIF-8 films are formed on both sides of the membrane.[142] The contra-diffusion method could lead to the controllable thicknesses of MOF films, and the thicknesses can be tuned by the reaction time as well as the metal ions (ligands ratio in the reaction system).[272] Actually, this part is similar to Section 3.1.2. Hence no further details are given here.

4.1.4 Layer-by-layer (LBL) method. The LBL method is also an effective method to obtain MOF films, in which the substrates are placed in the solution in a stepwise way.[6] A typical scheme of the LBL method is shown in Fig. 30. According to this method, MOF thin films could be constructed by depositing alternating layers of oppositely charged material. The detailed parameters could vary according to the types of MOFs. Interestingly, a polydopamine (PDA) layer which can work as a nucleation centre for MOFs is discovered and studied. PDA can be compactly formed on any types of solid surfaces and can work as an effective and valid nucleation centre for the deposition of MOF thin films. As for the preparation of MOF films, there are two issues that need to be considered, namely obtaining sufficient bond strength between polymer fibres and MOFs and effective deposition of MOFs. Four polymer films were chosen as substrates for the deposition of MOF materials, namely polystyrene (PS), polyethylene (PE), polypropylene (PP) and polyvinylidene fluoride (PVDF). The PDA modification of the substrate can be accomplished by immersing this type of substrate in a weakly basic dopamine HCl solution. The MOF was deposited on the modified polymer film using the LBL method. Since the catechol group on the PDA coating has a strong coordination ability with metal ions, the catechol group can be combined with metal ions. The MOF can be deposited on the substrate by synthesizing the MOF based on the coordination of the metal ions and the check group. MIL-100 (Fe), MOF-5, HKUST-1, and ZIF-8 were deposited on the modified substrate, respectively. Taking PP as an example, their SEM images are given (Fig. 31).[273] The LBL method may lead to the good control of layer thickness and give rise to oriented films.[274–278] However, the LBL method can only be used to prepare particular types of MOF thin films, which limits its application.[121]

4.1.5 Hot-pressing method. The hot-pressing (HoP) method can produce MOF films without a binder and solvent. The precursor of MOFs is connected with the functional group

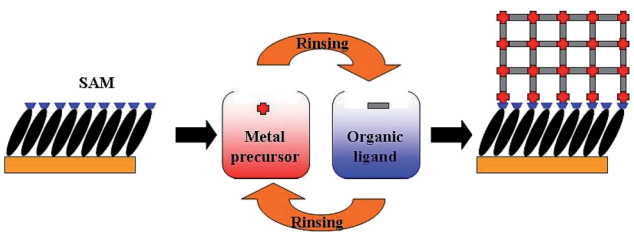

Fig. 30 Illustration of the synthesis of MOF films using the LBL method.[279]

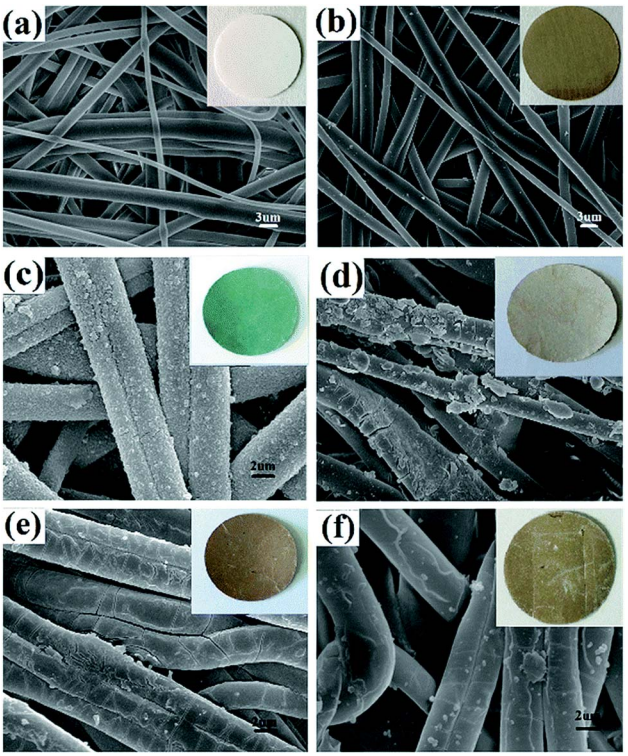

Fig. 31 The SEM images of the (a) pristine PP membrane, (b) PP membrane modified with PDA, and the SEM of modified PP membranes deposited with (c) HKUST-1, (d) MOF-5, (e) MIL-100(Fe), and (f) ZIF-8.[273] Copyright 2015, Royal Society of Chemistry.

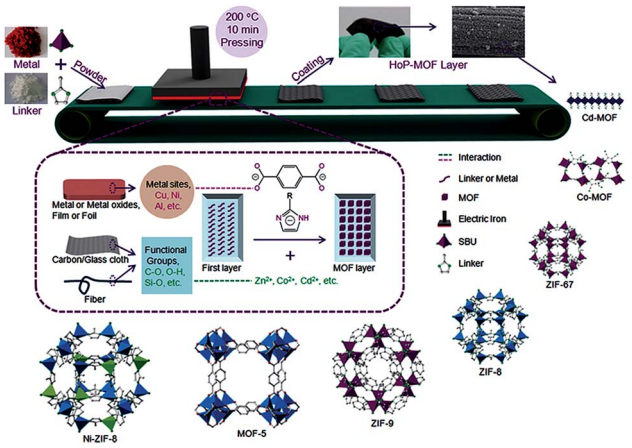

Fig. 32 HoP method for the preparation of various MOF thin films.[280] Copyright © 2016 John Wiley & Sons, Inc.

of the substrates at high temperature (probably by heating with an electric iron), and then MOF films begin to grow on the substrates.[6] The HoP method can grow MOFs on flexible materials and is expected to be applied to flexible electronic devices.[280] Chen *et al.* used the HoP method to prepare MOFs under both solvent-free and binder-free conditions. Controlling the temperature and pressure of the reaction, organic linkers, metal ions, or MOF precursors can react with metal sites or surface functional groups on the substrate as a basis for the growth of MOFs on the substrate. Taking ZIF-8 as an example, a mixed powder of $Zn(OAc)_2$, polyethylene glycol (PEG) and 2-methylimidazole is evenly coated on carbon cloth and wrapped in aluminum foil. ZIF-8 coated carbon cloth can be obtained by heating with an electric iron. By the same strategy, ZIF-9, ZIF-67, Ni-ZIF-8, Co-MOF, Cd-MOF and MOF-5 were successfully coated on carbon cloth (Fig. 32). Moreover, the successful preparation of the Ni-ZIF-8 coating shows that this method is beneficial to the preparation of mixed metal MOF coatings. The HoP method can produce a uniform MOF coating and maintain the original microporosity and crystallinity of the MOF,[280] and avoid the use of solvent. However, this method has a high requirement for the thermal stability of MOFs.

4.1.6 Liquid-phase epitaxy approach. As an efficient strategy to obtain oriented and well-defined MOF thin films based on various substrates, the LPE method has been developed several years ago. In this method, MOF crystals are precipitated from solution and then deposited on a substrate to form a thin layer of single crystals.[87,281] Detailed procedures of the LPE method are mentioned in Section 3.1.3. Many MOF films have been synthesized *via* the LPE method in many recent reports.[282] A spray LPE method was used to prepare an electronically conductive MOF, namely $Cu_3(HHTP)_2$, where HHTP refers to 2,3,6,7,10,11-hexahydroxytriphenylene. Ethanol and solutions of $Cu(OAc)_2$ and HHTP are alternately sprayed on the surface of the substrate to obtain a thin film. The number of layers can be decided by the control of the spraying times.[283]

The LPE method is used in some studies to construct special thin films. The encapsulation of guest molecules into the structure of MOF thin films could be achieved *via* the LPE method. A *trans*-azobenzene@HKUST-1 thin film was prepared by immersing substrates in copper acetate solution, BTC solution, and *trans*-azobenzene solution successively. A hundred cycles were used to prepare the *trans*-azobenzene@HKUST-1 thin film.[284] Lanthanide coordination compounds were also encapsulated into HKUST-1 thin films *via* the LPE method.[285] Eddaoudi *et al.* have grown Cu-tbo-MOF-5 on HKUST-1 and obtained a MOF-on-MOF heterostructure with hierarchical porosity, which exhibits [001] directional growth.[286]

Especially, 2D MOFs and MOF thin films for quartz crystal microbalance (QCM) sensors are usually prepared *via* the LPE method. A QCM is helpful for the estimation of the sorption performances of MOF thin films.[287] Fischer *et al.* developed a direct growth strategy of MOF thin films on the surface of QCM sensors *via* the LPE method, which allows the adsorption performances of the heterostructures to be able to probed in real time, indicating the important role that the matrix plays in MOF thin films.[288] Furukawa *et al.* prepared sophisticated heterostructured non-centrosymmetric binary Janus 2D-MOF coatings based on a QCM.[289] The LPE method is popular for the preparation of MOF thin films because of the simple synthetic procedure and high growth rate. Additionally, highly crystalline and oriented MOF thin films could be obtained *via* this method,[87,290,291] and it also enables great control of the film thickness and compositions of films along the vertical direction.[286] The LPE method could also give rise to MOF thin films with the potential for optical sensing.[292,293]

4.1.7 Spin coating method. MOF films can be prepared *via* the spin coating method. A matrix is placed on a spinning surface, and different precursor solutions are dropped on the centre of the matrix. Precursor solutions are thrown centrifugally towards the side of the matrix, and uniformly coat it. According to a previous report, Chernikova *et al.* proposed a spin coating method based on the liquid-phase epitaxy approach, which can lead to thin and smooth MOF films in a short time. The coating was performed using a fully automatic spin coater equipped with 4 micro-syringes (Fig. 33). First, a solution containing metal ions is added dropwise using a syringe. As the device is in rotation, the solution can be uniformly distributed throughout the substrate surface. Then, the solvent is added dropwise using the syringe to wash the substrate. Repeating the above process can achieve the coating of the organic linker. These four steps are considered as one cycle. The thickness of the film can be increased after multiple cycles. In the preparation process, the spin-coating time, spin-coating speed and injection volume/concentration may affect the coating effect. According to this method, $Cu_2(bdc)_2 \cdot xH_2O$, $Zn_2(bdc)_2 \cdot xH_2O$, HKUST-1, and ZIF-8 films have been successfully prepared. This method can be used to construct MOF films whose thickness ranges in from the micron scale to the nanoscale. Especially, this method can shorten the reaction time, reduce the reactant consumption and effectively reduce costs.[294] Similarly, some other studies also used this strategy.[295] In fact, as a mature technology, the spin coating method is used in many other reports.[296] The spin coating method could give rise to coatings with a high density and uniform thickness, despite the defects of crystals it might cause.

4.1.8 Atomic layer deposition (ALD) method. Atomic layer deposition (ALD) is a technique where two precursors are respectively blown onto the surface of the substrate with a pulse of gas to form a thin film. It could give rise to ultrathin and uniform MOF films. The excess precursor is further blown out by using an inert gas. The same process is repeated for another precursor. A film could be constructed *via* repeating the steps mentioned above.[297,298] UiO-66 is one of the most stable MOFs and was first successfully prepared by Cavka *et al.*[299] Therefore, UiO-66 is suitable to prepare the film. Thin film deposition of UiO-66 in an all-vapor phase process has been reported. This deposition is achieved by ALD. The continuous reaction of 1,4-benzenedicarboxylic acid and $ZrCl_4$ produces an organic–inorganic hybrid film. The film is subsequently crystallized into a UiO-66 crystal structure in acetic acid vapor.[297] As an important method to obtain MOF thin films, ALD is an efficient strategy to achieve the control of localized MOF thin film formation.[300]

4.1.9 Template growth method. The template growth method could be regarded as an efficient method to prepared MOF films with preferred crystalline orientation and other special properties. Some templates, such as linear polymers, could act as the template to guide the growth of MOF thin films and further endow them with high orientation. Different types of templates have been used to construction MOF thin films, which will be discussed below.

According to some researches, MOF thin films could be prepared assisted by some oriented linear species. MOF layers could be deposited on the matrix in the direction of the linear species. Typically, nanowires and surfactant could be used as the linear species in this method. The surfactant-assisted synthetic method refers to the use of a surfactant to guide the deposition direction of the film so that the formed film has anisotropy (Fig. 34). Typically, Wang *et al.* used a heme-like ligand, TCPP (Fe) (Fe(III) tetra(4-carboxyphenyl)porphine chloride), for the first time to synthesize an ultra-thin 2D MOF. Then the deposition of 2D MOFs leads to a MOF film. Co-TCPP (Fe), Cu-TCPP (Fe), and Zn-TCPP (Fe) nanosheets can be prepared using the surfactant-assisted synthetic method. These nanosheets can be deposited on the electrode as multilayer films by the Langmuir–Schäfer method. It can be used as a chemical sensor for detecting H_2O_2.[301] Similar to the surfactant-assisted synthetic method, different IRMOFs prepared with the assistance of zinc oxide nanowires have been reported. Zinc oxide nanowires have been grown on the substrate before the nanowire substrate is immersed in the IRMOF precursor solution. The resulting film is highly crystalline and the out-of-plane

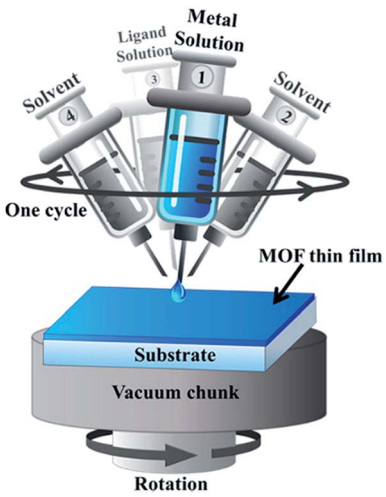

Fig. 33 Schematic representation of the coating process.[294] Copyright 2016, American Chemical Society.

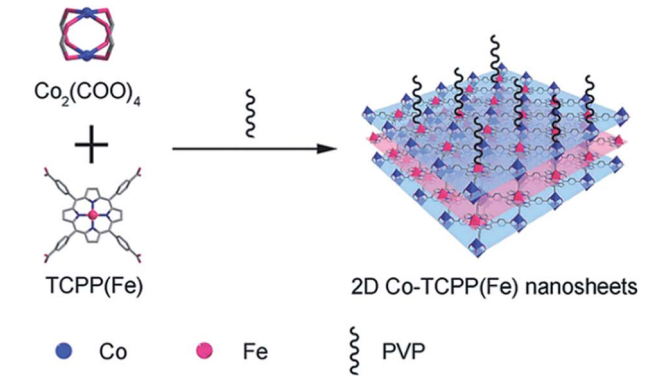

Fig. 34 The surfactant-assisted synthesis of Co-TCPP(Fe) nanosheets.[301] Copyright © 2016 John Wiley & Sons, Inc.

orientation varies with the type of IRMOF. IRMOF-1 and IRMOF-3 exhibit the (220) orientation while IRMOF-9 exhibits the (111) orientation.[302] This method could lead to highly crystalline MOF thin films.

A templated growth method was developed to prepare free-standing thin films based on porous coordination networks (PCNs),[303,304] namely PCN-221, PCN-222 and PCN-223. According to the report, H_6TCPP, $ZrCl_4$, and acetic acid (orbenzoic acid) are dissolved in *N*,*N*-dimethylformamide in different proportions. The solution is heated to prepare different PCN thin films on various substrates, such as flat surfaces, inclined/curved supports, complex 3D-printed objects and the inner walls of hollow pipes. The thin film could be detached by soaking it in acetone and activated by dissolving in DMF and heating. PCN thin films with various shapes could be obtained in this study.[305]

4.1.10 Femtosecond pulsed-laser deposition method. Since the manufacture and modification methods of MOF films based on chemical means have been developed,[306] physical deposition relatively has not been used very widely. According to a report, a femtosecond pulsed-laser deposition (femto-PLD) method was developed to prepare MOF thin films, which extends MOF film fabrication methods to physical vapor deposition. The procedure of this method is shown in Fig. 35. In the study, ZIF-8 powder was immersed in PEG-400 (PEG = polyethylene glycol) for stabilization, and then the targets were prepared by pressing the immersed powder into a pellet. A PEG@ZIF-8 film was deposited onto a sapphire substrate at room temperature by the ablation of the target in a vacuum. Apparently, the pretreatment and ablation of the precursor are central steps in this strategy. According to a report, the femto-PLD strategy is suitable for the construction of thermally labile and highly porous MOF films because of the addition of stabilizing additives.[307]

4.2 Applications of MOF films

Unlike 2D MOFs, the thickness of MOF thin films is greater than that of atomic monolayers. For manufacture and practical applications, MOF thin films have the following advantages: (1) the MOFs are not restricted to the ones that have a 2D planar structure, indicative of the extensive sources of MOF films; (2) compared with 2D MOFs, the exfoliation process could be avoided, which simplifies the preparation; (3) the higher thickness probably endows MOF films with enhanced mechanical strength.

4.2.1 Sensor. Apart from 2D MOFs, MOF thin films could also be used as sensors. Luminescence was defined as the emission of light caused by energy absorption.[308] MOF-based luminescent materials for sensing applications have been reviewed earlier.[309] Photoluminescence has attracted much attention because of its potential application in sensors. Just as mentioned earlier, the Eu-HBPTC film exhibits special photoluminescence properties. The luminescence properties of Eu-HBPTC films in DMF, water and CO_3^{2-} solution were investigated (Fig. 36). Both water and CO_3^{2-} solution can lead to the decrease of emission intensity. According to the report, this decrease is due to the replacement of DMF molecules by H_2O since the Eu-HBPTC film is synthesized in DMF solution and channels are filled by DMF molecules. Since the luminescence of the Eu-HBPTC film disappears with the existence of CO_3^{2-}, it can be used as a chemical sensor by simply coupling with a UV cash detector, which can help detect CO_3^{2-}.[270] In fact, lanthanide-based MOFs[270,310,311] and novel metal-based MOFs[312] usually exhibit apparent light-emitting performance, which endows them with the potential for application in sensors.

Design of the metal ion centre and ligand could apparently affect the luminescence of MOFs. Two types of CP films based on zig–zag Cu_2I_2 chains have been developed, which show reversible thermo/mechano-luminescence. The isonicotinate ligands in CPs were functionalized with amino groups, which further affects the symmetry of Cu_2I_2 and Cu–Cu distances.[313]

Fluorescence quenching phenomena were also employed for sensors in a number of research studies. Lanthanides which act as prominent emitting sites are mainly reported as "turn-on" or "turn-off" sensors, depending on intensity changes of the luminescence.[311] As one of the lanthanide elements, terbium

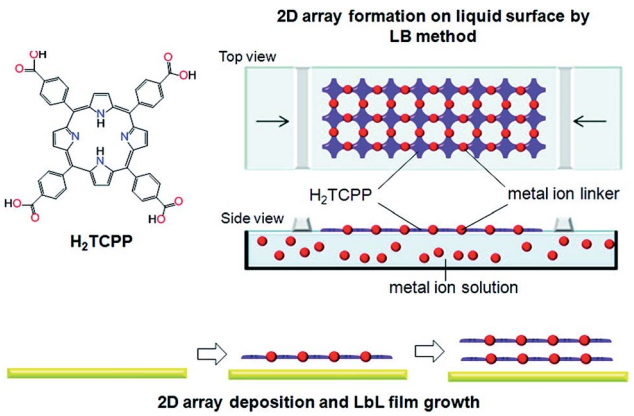

Fig. 35 Scheme of the fabrication of ZIF-8 by using the 2D array deposition and LBL film growth strategy.[307] Copyright 2017, American Chemical Society.

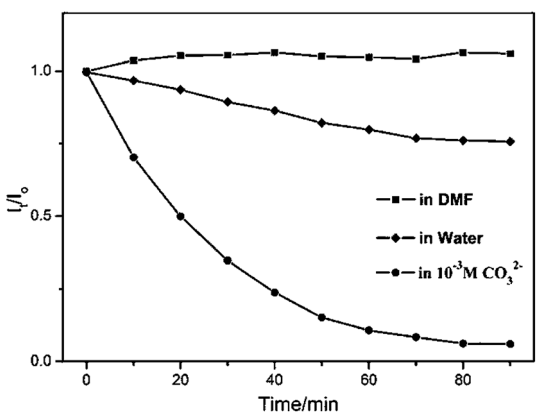

Fig. 36 The relationship between the ratio I_t/I_0 of the Eu-HBPTC film and time in different media, which reflects the luminescence intensity.[270] Copyright 2014, Royal Society of Chemistry.

could act as the metal ion centre in MOFs and endow MOFs with excellent performances in the application of sensors. A Tb-MOF thin film was developed *via* an electrodeposition method, which could act as the sensor of 2,4-dinitrotoluene (DNT). The MOF is able to detect DNT at concentrations of 0.1 mM (corresponding to circa 23 ppm) independently of the substrate used for the synthesis (Tb metal or TbOx). At a DNT concentration of <0.1 mM, the luminescence intensity of Tb(III) was quenched to 90% of the initial intensity, indicating a potential use of the Tb-MOF thin film as a sensor.[314] Hence lanthanide containing MOF thin films could be good candidates for tunable luminescent sensors. Besides, the combination between lanthanide elements and other metal elements could also lead to luminescent materials.[315] A 2D interdigitated architecture, $\{[Cd_2(sdb)_2(4\text{-bpmh})_2(H_2O)]\}_n \cdot 2n(H_2O)$ (sdb = 4,4′-sulfonyl dibenzoic acid, and 4-bpmh = *N*,*N*-bis-pyridin-4-ylmethylene-hydrazine), was prepared. A fluorescence quenching was observed after the addition of nitrobenzene, which may follow the fluorescence quenching mechanism. After the addition of 40 ppm (98%) of nitrobenzene, the luminescence intensity was completely quenched, and the fluorescence intensity almost recovered after five cycles. As is mentioned in the report, the fluorescence quenching could be attributed to the electron transfer from the MOF to electron deficient nitrobenzene through interspecies contact.[316]

Three MOFs, PCN-14, NOTT-100 and NOTT-101, are deposited on surface acoustic wave sensors, according to a previous report. These MOFs exhibit the "nbo" topology and have different space groups. These MOF-coated membrane sensors can respond reversibly to the vapours of acetone, *n*-hexane and water, which is shown in Fig. 37, and their responses are compared with that of HKUST-1. In fact, all four membranes respond to water vapor more sensitively than to organic compound vapours.[276] HKUST-1 was used to coat a plasmonic substrate to amplify the sensing signal of localized surface plasmon resonance spectroscopy, which was used as the sensor of CO_2 in the study.[317] Besides, some gas sensors towards NH_3,[283,318] O_2,[319] and H_2S[320] have also been developed until now.

4.2.2 Conductive devices. As mentioned earlier, the design of MOFs could result in improved conductive devices. However, integrating conductive ligands into MOFs to achieve conductivity and achieving selective attachment to the substrate surface are still difficult. The design of conductive MOF structures needs the measurement of the electronic structure, which can provide the feedback and instruction for the design process. Elzein *et al.* used a clean structural synthesis combined with photoemission spectroscopy in a vacuum system in a glove box to study the Frontier orbital structure of MOF films which is self-assembled. This research reveals the characterization of the interfacial electronic structure which is composed of polymeric materials and conductive small molecules. Suitable metal ions and organic linkers can be selected and decided *via* this measurement technology.[321]

Talin *et al.* designed a HKUST-1 thin film with tunable electrical conductivity. The HKUST-1 film was grown on silicon wafers which were covered with SiO_2 and prepatterned with Pt pads. Then the film was infiltrated with 7,7,8,8-tetracyanoquinodimethane (TCNQ), redox-active and conjugated guest molecules. The conductivity is caused by TCNQ guest molecules bridging binuclear copper paddlewheels, which leads to apparent electronic coupling between dimeric Cu subunits.[322]

In addition, in order to improve the conductivity of MOFs, a blue pillared-paddle wheel MOF film was constructed on a ZnO substrate, and π-acidic methyl viologen guests infiltrated the film. After the infiltration, the electrical conductivity of the MOF film rose from *ca.* 6×10^{-5} S m^{-1} (25 °C) to 2.3×10^{-3} S m^{-1}, indicating that the complementary guest π-systems could tune the conductivity of MOFs, because the complementary π-systems can give rise to long-range electron delocalization.[323]

4.2.3 Switch device. Liu *et al.* introduced the resistance conversion properties of MOF films in alcohol-mediated and memory devices. An alcohol-mediated multi-resistor switch device based on ZIF-8 was proposed (Fig. 38a). ZIF-8 films were placed between the electrodes to set up Ag/ZIF-8/Si structures. Alcohol vapors are exploited to explore and verify chemically mediated memory effects. ZIF-8 (Fig. 38b) has permanent porosity and high thermal stability and chemical stability and can therefore be used to fabricate memory devices. Atomic force microscopy (AFM) and SEM images of this film are shown in Fig. 38. Studies have shown that the ordered arrangement of hydrogen bonding systems and guest molecules in MOF crystals leads to dielectric conversion of alcohols. Such a memory device

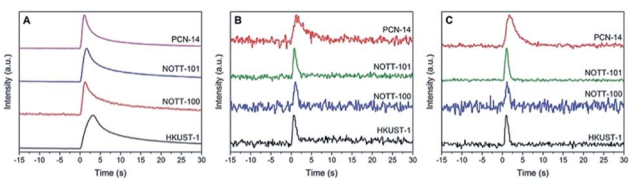

Fig. 37 The phase shift intensity *versus* experimental time for surface acoustic wave sensors which are coated with NOTT-100, NOTT-101, PCN-14 and HKUST-1 upon the injection of (A) water, (B) acetone and (C) *n*-hexane.[276] Copyright © 2016 John Wiley & Sons, Inc.

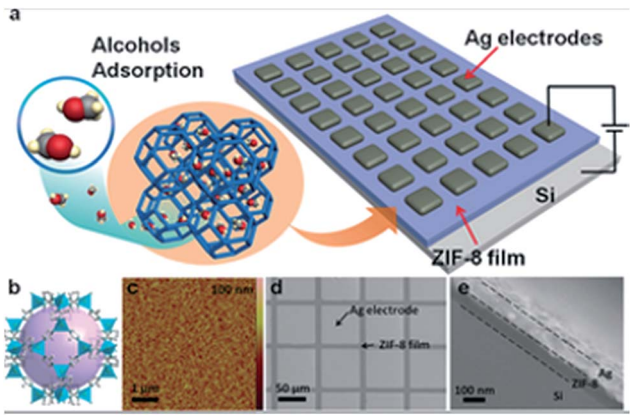

Fig. 38 (a) The diagram of the alcohol-mediated resistance-switching device; (b) the diagram of the structure of ZIF-8; (c) AFM image of the ZIF-8 film on silica; (d) SEM image of the device from the top view; (e) SEM image of the device from the cross view.[324] Copyright © 2016 John Wiley & Sons, Inc.

is expected to be made into an environmental response device, and it has a bright future in a wearable information storage system. It is worth noting that if such a MOF film is coated on a flexible substrate, it can be used in a flexible electronic device.[324]

A resistance switching random access memory (ReRAM) device was designed by introducing a ZIF-8 thin film prepared by the solvothermal method as a resistance switching layer. The ZIF-8 thin film was stacked in between Al and Au thin films, which act as the top and bottom electrodes respectively, and the film exhibited a resistive switching behavior under a DC voltage sweep, indicating its potential programmable memory properties.[325]

4.2.4 Catalysis. Apart from 2D MOFs among 2D-architectured MOFs, MOF thin films also exhibit catalytic activity towards CO_2 reduction, degradation of pollutants and so on. The treatment of carbon dioxide is crucial to solve the greenhouse effect and energy crisis. Apart from the separation of CO_2 from gas mixtures, some catalysts can also be applied to promote the reduction of CO_2. Li and colleagues have proved that electrons which are produced by semiconductor moieties can be transferred to MOF moieties so they can participate in photocatalytic reactions. Thus, the combination between MOFs and semiconductor nanoparticles can lead to favorable catalysts. Maina and co-workers encapsulated Cu–TiO_2 and TiO_2 nanoparticles into the pores of ZIF-8. They modified a stainless steel substrate with graphene oxide (GO) which serves as the substrate for the ZIF-8 film (Fig. 39a). This hybrid film shows photocatalytic activity for the reduction of MB under the irradiation of UV light. As shown in Fig. 39b, after the encapsulation of Cu–TiO_2 or TiO_2 nanoparticles, the photocatalytic activity is improved apparently. Besides, the relationship between photocatalytic properties and the content of Cu–TiO_2 is also studied, and is shown in Fig. 39c.[326] The photoactive triphenylamine moiety was incorporated to construct a Gd-MOF film based on an α-Al_2O_3 plate, which exhibits considerable photocatalytic activity towards the reduction of CO_2. The α-Al_2O_3 plate could prolong the lifetime of the catalytic system because of the combination between the large surface areas of

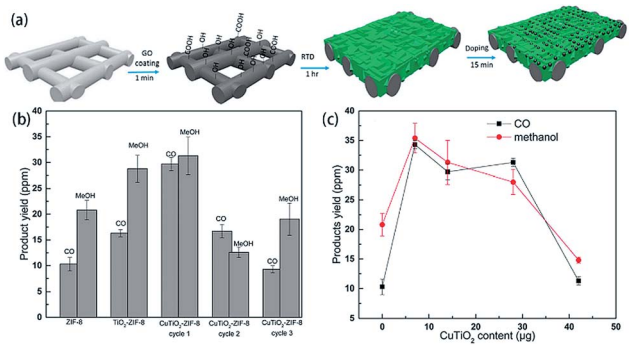

Fig. 39 (a) The modification of a substrate and the encapsulation of semiconductor nanoparticles into MOF membranes. (b) The photocatalytic activities of different membranes. (c) The relationship between photocatalytic activity and the content of Cu–TiO_2.[326] Copyright 2017, American Chemical Society.

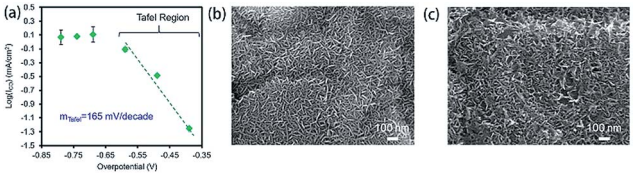

Fig. 40 (a) Tafel plot of partial current density for carbon oxide production. (b and c) The SEM images of MOF thin films before and after the reaction, respectively.[328] Copyright 2015, American Chemical Society.

α-Al_2O_3 plate and the high porosity of MOFs.[327] Yaghi and Yang *et al.*[328] examined the electrocatalytic activity of the Co-based MOF thin film towards the reduction of CO_2. The chemical formula of this MOF is $Al_2(OH)_2$TCPP-Co (TCPP-H_2 = 4,4′,4″,4-(porphyrin-5,10,15,20-tetrayl)tetrabenzoate). The MOF thin film was prepared by the ALD strategy. The active sites in molecular porphyrins are exposed to the electrolyte and linked to the support electrically, which enables the MOF thin film containing porphyrin moieties to be used as an electrocatalyst. CO_2 was reduced to CO in this study. The Tafel plot displayed in Fig. 40a shows a Tafel slope of 165 mV dec^{-1} in the low-overpotential region, indicating the probable rate-limiting step caused by the reduction of CO_2 to form a CO_2 radical. And the SEM images before and after the catalytic reaction suggest that the plate-like morphology of the MOF thin film has been retained during the reaction (Fig. 40b and c). It could be a promising electrocatalyst candidate towards the reduction of CO_2.

5. Conclusions

In this contribution, we have successively overviewed the synthetic strategies of 2D MOFs, MOF membranes and MOF thin films. These MOF-based materials could be prepared by some classical methods, such as solvent methods, LPE methods and so on; meanwhile, they can be obtained *via* many newly developed and novel strategies. By choosing the synthetic methods, MOF-based materials with various properties, such as flexibility and good orientation, could be obtained. Then the device applications of the aforementioned MOF-based materials have been summarized, which exhibit bright prospects in many fields.

However, as far as we are concerned, more efforts should be done in many future studies to obtain more improved MOF-based films. For instance, an important aspect is that the current studies of MOF membranes and thin films are mainly based on the MOFs with mature synthetic methods, such as ZIF-8 and HKUST-1. Some other MOFs, such as MOF-177,[329] are hardly used to prepare membranes and thin films. Thus, future research could aim at the synthetic strategies of membranes and films of those MOFs which haven't been prepared as membranes or thin films.

We can conclude that there are several ways to improve the stability and close combination of MOF membranes, which are (1) applying sonication to the synthesis of membranes,[133] (2) introducing amine groups into MOFs so as to form covalent linking,[137] and (3) doping MOFs with rare earth element and

combining MOFs with some organic solvents such as polymers and gel materials.[330–332] We can get inspiration from many existing studies to obtain improved 2D MOFs, MOF membranes, MOF thin films and devices.

The strategies for other kinds of MOF materials are also able to be extended to the application of MOF membranes. Apart from the matrices we mentioned before, some special substrates can be used to improve the adsorption capacity of MOFs, such as marine sponges[333] and diatoms.[334] In fact, Morph-Genetic MOFs should be paid more attention to. Patterned MOF thin films have been prepared *via* various methods,[265,271,335] and we should pay more attention to their potential for barcodes and many other applications. Mesoporous MOFs should also be paid attention to, because of their bright prospects for the discovery of various applications.[336] From the selectivity MOF regulators proposed by Zhao *et al.*,[337] MOF membranes can be designed as catalytic reaction regulators based on gully or porous substrates. Interestingly, a hierarchical MOF-on-MOF structure has been prepared, which could be helpful for the construction of MOF-based MOF membranes.[338] A COF-on-MOF structure has also been developed and exhibits excellent photocatalytic activity towards the degradation of organic pollutants.[339] All in all, as far as we are concerned, the further effort on MOF thin films, membranes and 2D MOFs to construct new types of membranes and obtain MOFs or composites with improved properties could be aimed at: (1) the combination between MOFs and COFs or different kinds of MOFs; (2) the use of sacrificial templates for the construction of MOF membranes; (3) the control of the mechanical properties; (4) the preparation of patterned MOF thin films *via* electrochemical deposition, template guidance or other strategies. Besides, there are still some applications of MOF thin films, membranes and 2D MOFs that aren't covered in our review, such as breathing MOFs,[340] supercapacitors,[341–347] dielectric materials,[348] barcode systems,[271,349] and osteogenic and antibacterial effects,[350] which require more in-depth studies. MOF membranes, thin films and 2D MOFs have bright prospects in device applications, but still require more studies.

Conflicts of interest

There are no conflicts to declare.

Acknowledgements

This work was supported by the National Natural Science Foundation of China (Grant No. 51603052), the Special Funds for Scientific and Technological Innovation and Cultivation of Guangdong University Students (Grant No. pdjh2019b0019), and the Fundamental Research Funds for the Central Universities (Grant No. 18lgpy02). H. L. Zhu especially wishes to thank Yi Xiang for support.

Notes and references

1 O. M. Yaghi, G. Li and H. Li, *Nature*, 1995, **378**, 703.
2 J. Choi, J. Park, M. Park, D. Moon and M. S. Lah, *Eur. J. Inorg. Chem.*, 2008, **2008**, 5465.
3 Y. X. Xie, W. N. Zhao, G. C. Li, P. F. Liu and L. Han, *Inorg. Chem.*, 2016, **55**, 549.
4 L. Pan, G. Liu, H. Li, S. Meng, L. Han, J. Shang, B. Chen, A. E. Platero-Prats, W. Lu, X. Zou and R. W. Li, *J. Am. Chem. Soc.*, 2014, **136**, 17477.
5 Y. Z. Zhang, T. Cheng, Y. Wang, W. Y. Lai, H. Pang and W. Huang, *Adv. Mater.*, 2016, **28**, 5242.
6 Y. Li, B. Zou, A. Xiao and H. Zhang, *Chin. J. Chem.*, 2017, **35**, 1501.
7 P. Davydovskaya, A. Ranft, B. V. Lotsch and R. Pohle, *Anal. Chem.*, 2014, **86**, 6948.
8 B. Li, H. M. Wen, Y. Cui, W. Zhou, G. Qian and B. Chen, *Adv. Mater.*, 2016, **28**, 8819.
9 J. D. Rocca, D. Liu and W. Lin, *Acc. Chem. Res.*, 2011, **44**, 957.
10 Y. Chen, X. Huang, S. Zhang, S. Li, S. Cao, X. Pei, J. Zhou, X. Feng and B. Wang, *J. Am. Chem. Soc.*, 2016, **138**, 10810.
11 M. X. Wu and Y. W. Yang, *Adv. Mater.*, 2017, **29**, 1606134.
12 V. Stavila, A. A. Talin and M. D. Allendorf, *Chem. Soc. Rev.*, 2014, **43**, 5994.
13 Y. Xie, Z. Yu, X. Huang, Z. Wang, L. Niu, M. Teng and J. Li, *Chemistry*, 2007, **13**, 9399.
14 J. J. Perry Iv, J. A. Perman and M. J. Zaworotko, *Chem. Soc. Rev.*, 2009, **38**, 1400.
15 O. K. Farha and J. T. Hupp, *Acc. Chem. Res.*, 2010, **43**, 1166.
16 Y. Cui, B. Li, H. He, W. Zhou, B. Chen and G. Qian, *Acc. Chem. Res.*, 2016, **49**, 483.
17 W. Lu, Z. Wei, Z.-Y. Gu, T.-F. Liu, J. Park, J. Park, J. Tian, M. Zhang, Q. Zhang, T. Gentle Iii, M. Bosch and H.-C. Zhou, *Chem. Soc. Rev.*, 2014, **43**, 5561.
18 Z. W. Mo, H. L. Zhou, D. D. Zhou, R. B. Lin, P. Q. Liao, C. T. He, W. X. Zhang, X. M. Chen and J. P. Zhang, *Adv. Mater.*, 2018, **30**, 1704350.
19 O. M. Yaghi, M. O'Keeffe, N. W. Ockwig, H. K. Chae, M. Eddaoudi and J. Kim, *Nature*, 2003, **423**, 705.
20 U. Mueller, M. Schubert, F. Teich, H. Puetter, K. Schierle-Arndt and J. Pastré, *J. Mater. Chem.*, 2006, **16**, 626.
21 X.-Y. Cui, Z.-Y. Gu, D.-Q. Jiang, Y. Li, H.-F. Wang and X.-P. Yan, *Anal. Chem.*, 2009, **81**, 9771.
22 J. J. Bodwin and V. L. Pecoraro, *Inorg. Chem.*, 2000, **39**, 3434.
23 M. Eddaoudi, D. B. Moler, H. Li, B. Chen, T. M. Reineke, M. O'Keeffe and O. M. Yaghi, *Acc. Chem. Res.*, 2001, **34**, 319.
24 A. Ambrosi, C. K. Chua, A. Bonanni and M. Pumera, *Chem. Rev.*, 2014, **114**, 7150.
25 M. J. Allen, V. C. Tung and R. B. Kaner, *Chem. Rev.*, 2010, **110**, 132.
26 Y. Chen, Z. Fan, Z. Zhang, W. Niu, C. Li, N. Yang, B. Chen and H. Zhang, *Chem. Rev.*, 2018, **118**, 6409.
27 A. F. Khan, D. A. C. Brownson, E. P. Randviir, G. C. Smith and C. E. Banks, *Anal. Chem.*, 2016, **88**, 9729.
28 D.-Q. Hoang, P. Pobedinskas, S. S. Nicley, S. Turner, S. D. Janssens, M. K. Van Bael, J. D'Haen and K. Haenen, *Cryst. Growth Des.*, 2016, **16**, 3699.

29 Z. Wang, Q. Jingjing, X. Wang, Z. Zhang, Y. Chen, X. Huang and W. Huang, *Chem. Soc. Rev.*, 2018, **47**, 6128.
30 M. Zhao, Y. Huang, Y. Peng, Z. Huang, Q. Ma and H. Zhang, *Chem. Soc. Rev.*, 2018, **47**, 6267.
31 S. Furukawa, J. Reboul, S. Diring, K. Sumida and S. Kitagawa, *Chem. Soc. Rev.*, 2014, **43**, 5700.
32 A. C. Sudik, A. P. Côté, A. G. Wong-Foy, M. O'Keeffe and O. M. Yaghi, *Angew. Chem., Int. Ed.*, 2006, **45**, 2528.
33 C. Zhang, Y. Xiao, D. Liu, Q. Yang and C. Zhong, *Chem. Commun.*, 2013, **49**, 600.
34 H. Zhu, D. Liu, D. Zou and J. Zhang, *J. Mater. Chem. A*, 2018, **6**, 6130.
35 G. Zhong, D. Liu and J. Zhang, *J. Mater. Chem. A*, 2018, **6**, 1887.
36 M. Dan-Hardi, C. Serre, L. R. Théo Frot, G. Maurin, C. m. Sanchez and G. r. Férey, *J. Am. Chem. Soc.*, 2009, **131**, 10857.
37 A. Salinas-Castillo, A. J. Calahorro, D. Briones, D. Fairen-Jiménez, F. Gándara, C. Mendicute-Fierro, J. M. Seco, M. Pérez-Mendoza, B. Fernández and A. Rodríguez-Diéguez, *New J. Chem.*, 2015, **39**, 3982.
38 J. Gascon and F. Kapteijn, *Angew. Chem., Int. Ed.*, 2010, **49**, 1530.
39 R. Ricco, L. Malfatti, M. Takahashi, A. J. Hill and P. Falcaro, *J. Mater. Chem. A*, 2013, **1**, 13033.
40 C.-Y. Liu, H.-T. Wang, W.-C. Chung, Y.-T. Cheng, Y.-T. Chen, M.-L. Ho, C.-C. Wang, G.-H. Lee and H.-S. Sheu, *J. Chin. Chem. Soc.*, 2012, **59**, 1070.
41 P. Falcaro, R. Ricco, C. M. Doherty, K. Liang, A. J. Hill and M. J. Styles, *Chem. Soc. Rev.*, 2014, **43**, 5513.
42 C. M. Liu, D. Q. Zhang, X. Hao and D. B. Zhu, *Sci. Rep.*, 2017, **7**, 11156.
43 L. Sun, M. G. Campbell and M. Dincă, *Angew. Chem., Int. Ed.*, 2016, **55**, 3566.
44 W. Li, L. Sun, J. Qi, P. Jarillo-Herrero, M. Dinca and J. Li, *Chem. Sci.*, 2017, **8**, 2859.
45 Q. Y. Yang, K. Li, J. Luo, M. Pan and C. Y. Su, *Chem. Commun.*, 2011, **47**, 4234.
46 D. G. Kurth and M. Higuchi, *Soft Matter*, 2006, **2**, 915.
47 A. M. Spokoyny, D. Kim, A. Sumrein and C. A. Mirkin, *Chem. Soc. Rev.*, 2009, **38**, 1218.
48 D. Rodríguez-San-Miguel, P. Amo-Ochoa and F. Zamora, *Chem. Commun.*, 2016, **52**, 4113.
49 X. Ouyang, Z. Chen, X. Liu, Y. Yang, M. Deng, L. Weng, Y. Zhou and Y. Jia, *Inorg. Chem. Commun.*, 2008, **11**, 948.
50 J. Lopez-Cabrelles, S. Manas-Valero, I. J. Vitorica-Yrezabal, P. J. Bereciartua, J. A. Rodriguez-Velamazan, J. C. Waerenborgh, B. J. C. Vieira, D. Davidovikj, P. G. Steeneken, H. S. J. van der Zant, G. Minguez Espallargas and E. Coronado, *Nat. Chem.*, 2018, **10**, 1001.
51 L.-Z. Yang, J. Wang, A. M. Kirillov, W. Dou, C. Xu, R. Fang, C.-L. Xu and W.-S. Liu, *CrystEngComm*, 2016, **18**, 6425.
52 D. J. Ashworth and J. A. Foster, *J. Mater. Chem. A*, 2018, **6**, 16292.
53 R. Dong, M. Pfeffermann, H. Liang, Z. Zheng, X. Zhu, J. Zhang and X. Feng, *Angew. Chem., Int. Ed.*, 2015, **54**, 12058.
54 R. Dong, Z. Zheng, D. C. Tranca, J. Zhang, N. Chandrasekhar, S. Liu, X. Zhuang, G. Seifert and X. Feng, *Chemistry*, 2017, **23**, 2255.
55 S. Motoyama, R. Makiura, O. Sakata and H. Kitagawa, *J. Am. Chem. Soc.*, 2011, **133**, 5640.
56 R. Makiura, S. Motoyama, Y. Umemura, H. Yamanaka, O. Sakata and H. Kitagawa, *Nat. Mater.*, 2010, **9**, 565.
57 P. Z. Li, Y. Maeda and Q. Xu, *Chem. Commun.*, 2011, **47**, 8436.
58 P. Amo-Ochoa, L. Welte, R. Gonzalez-Prieto, P. J. Sanz Miguel, C. J. Gomez-Garcia, E. Mateo-Marti, S. Delgado, J. Gomez-Herrero and F. Zamora, *Chem. Commun.*, 2010, **46**, 3262.
59 H. S. Quah, L. T. Ng, B. Donnadieu, G. K. Tan and J. J. Vittal, *Inorg. Chem.*, 2016, **55**, 10851.
60 J. A. Foster, S. Henke, A. Schneemann, R. A. Fischer and A. K. Cheetham, *Chem. Commun.*, 2016, **52**, 10474.
61 D. J. Ashworth, A. Cooper, M. Trueman, R. W. M. Al-Saedi, L. D. Smith, A. Meijer and J. A. Foster, *Chemistry*, 2018, **24**, 17986.
62 V. Nicolosi, M. Chhowalla, M. G. Kanatzidis, M. S. Strano and J. N. Coleman, *Science*, 2013, 340.
63 A. Abhervé, S. Mañas-Valero, M. Clemente-León and E. Coronado, *Chem. Sci.*, 2015, **6**, 4665.
64 R. Dai, F. Peng, P. Ji, K. Lu, C. Wang, J. Sun and W. Lin, *Inorg. Chem.*, 2017, **56**, 8128.
65 B. J. Burnett, P. M. Barron, C. Hu and W. Choe, *J. Am. Chem. Soc.*, 2011, **133**, 9984.
66 C. S. Diercks and O. M. Yaghi, *Science*, 2017, 355.
67 M. Li, D. Li, M. O'Keeffe and O. M. Yaghi, *Chem. Rev.*, 2014, **114**, 1343.
68 H.-L. Jiang, T. A. Makal and H.-C. Zhou, *Coord. Chem. Rev.*, 2013, **257**, 2232.
69 F.-Q. Wang, X.-J. Zheng, Y.-H. Wan, C.-Y. Sun, Z.-M. Wang, K.-Z. Wang and L.-P. Jin, *Inorg. Chem.*, 2007, **46**, 2956.
70 S. T. Hyde, B. Chen and M. O'Keeffe, *CrystEngComm*, 2016, **18**, 7607.
71 H. Furukawa, K. E. Cordova, M. O'Keeffe and O. M. Yaghi, *Science*, 2013, **341**, 1230444.
72 Z.-Q. Shi, Y.-Z. Li, Z.-J. Guo and H.-G. Zheng, *Cryst. Growth Des.*, 2013, **13**, 3078.
73 D. Zhao, D. J. Timmons, D. Yuan and H.-C. Zhou, *Acc. Chem. Res.*, 2011, **44**, 123.
74 C.-C. Wang, G.-B. Sheu, S.-Y. Ke, C.-Y. Shin, Y.-J. Cheng, Y.-T. Chen, C.-H. Cho, M.-L. Ho, W.-T. Chen, R.-H. Liao, G.-H. Leec and H.-S. Sheu, *CrystEngComm*, 2015, **17**, 1264.
75 I. M. Hauptvogel, V. Bon, R. Grunker, I. A. Baburin, I. Senkovska, U. Mueller and S. Kaskel, *Dalton Trans.*, 2012, **41**, 4172.
76 J. Guo, J.-F. Ma, B. Liu, W.-Q. Kan and J. Yang, *Cryst. Growth Des.*, 2011, **11**, 3609.
77 K. Kim, S. Park, K.-M. Park and S. S. Lee, *Cryst. Growth Des.*, 2011, **11**, 4059.
78 W.-H. Huang, L. Hou, B. Liu, L. Cui, Y.-Y. Wang and Q.-Z. Shi, *Inorg. Chim. Acta*, 2012, **382**, 13.
79 F. B. de Almeida, F. H. e Silva, M. I. Yoshida, H. A. de Abreu and R. Diniz, *Inorg. Chim. Acta*, 2013, **402**, 60.

80 F. Meng, L. Qin, M. Zhang and H. Zheng, *CrystEngComm*, 2014, **16**, 698.
81 X. Hu, Z. Wang, B. Lin, C. Zhang, L. Cao, T. Wang, J. Zhang, C. Wang and W. Lin, *Chem.–Eur. J.*, 2017, **23**, 8390.
82 D. J. Wales, J. Grand, V. P. Ting, R. D. Burke, K. J. Edler, C. R. Bowen, S. Mintova and A. D. Burrows, *Chem. Soc. Rev.*, 2015, **44**, 4290.
83 Z. Hu, B. J. Deibert and J. Li, *Chem. Soc. Rev.*, 2014, **43**, 5815.
84 L. E. Kreno, K. Leong, O. K. Farha, M. Allendorf, R. P. Van Duyne and J. T. Hupp, *Chem. Rev.*, 2012, **112**, 1105.
85 Y. Cui, Y. Yue, G. Qian and B. Chen, *Chem. Rev.*, 2012, **112**, 1126.
86 R. B. Lin, S. Y. Liu, J. W. Ye, X. Y. Li and J. P. Zhang, *Adv. Sci.*, 2016, **3**, 1500434.
87 O. Shekhah, J. Liu, R. A. Fischer and C. Wöll, *Chem. Soc. Rev.*, 2011, **40**, 1081.
88 Y. N. Wu, F. Li, W. Zhu, J. Cui, C. A. Tao, C. Lin, P. M. Hannam and G. Li, *Angew. Chem., Int. Ed.*, 2011, **50**, 12518.
89 Y. Hong, J. W. Y. Lam and B. Z. Tang, *Chem. Soc. Rev.*, 2011, **40**, 5361.
90 E. P. J. Parrott, N. Y. Tan, R. Hu, J. A. Zeitler, B. Z. Tang and E. Pickwell-MacPherson, *Mater. Horiz.*, 2014, **1**, 251.
91 M. Zhang, G. Feng, Z. Song, Y. P. Zhou, H. Y. Chao, D. Yuan, T. T. Tan, Z. Guo, Z. Hu, B. Z. Tang, B. Liu and D. Zhao, *J. Am. Chem. Soc.*, 2014, **136**, 7241.
92 I. Stassen, N. Burtch, A. Talin, P. Falcaro, M. Allendorf and R. Ameloot, *Chem. Soc. Rev.*, 2017, **46**, 3185.
93 S. Horike, D. Umeyama and S. Kitagawa, *Acc. Chem. Res.*, 2013, **46**, 2376.
94 A. Morozan and F. Jaouen, *Energy Environ. Sci.*, 2012, **5**, 9269.
95 S. Han, S. C. Warren, S. M. Yoon, C. D. Malliakas, X. Hou, Y. Wei, M. G. Kanatzidis and B. A. Grzybowski, *J. Am. Chem. Soc.*, 2015, **137**, 8169.
96 F. Wang, X. Wu, X. Yuan, Z. Liu, Y. Zhang, L. Fu, Y. Zhu, Q. Zhou, Y. Wu and W. Huang, *Chem. Soc. Rev.*, 2017, **46**, 6816.
97 S. Benmansour, A. Abherve, P. Gomez-Claramunt, C. Valles-Garcia and C. J. Gomez-Garcia, *ACS Appl. Mater. Interfaces*, 2017, **9**, 26210.
98 M. S. Denny Jr and S. M. Cohen, *Angew. Chem., Int. Ed.*, 2015, **54**, 9029.
99 A. J. Clough, J. M. Skelton, C. A. Downes, A. A. de la Rosa, J. W. Yoo, A. Walsh, B. C. Melot and S. C. Marinescu, *J. Am. Chem. Soc.*, 2017, **139**, 10863.
100 Y. He, C. D. Spataru, F. Leonard, R. E. Jones, M. E. Foster, M. D. Allendorf and A. Alec Talin, *Phys. Chem. Chem. Phys.*, 2017, **19**, 19461.
101 W. M. Liao, J. H. Zhang, S. Y. Yin, H. Lin, X. Zhang, J. Wang, H. P. Wang, K. Wu, Z. Wang, Y. N. Fan, M. Pan and C. Y. Su, *Nat. Commun.*, 2018, **9**, 2401.
102 B. Gómez-Lor, E. Gutiérrez-Puebla, M. Iglesias, M. A. Monge, C. Ruiz-Valero and N. Snejko, *Chem. Mater.*, 2005, **17**, 2568.
103 T. R. Cook, D. K. Dogutan, S. Y. Reece, Y. Surendranath, T. S. Teets and D. G. Nocera, *Chem. Rev.*, 2010, **110**, 6474.
104 R. D. L. Smith, M. S. Prévot, R. D. Fagan, Z. Zhang, P. A. Sedach, M. K. J. Siu, S. Trudel and C. P. Berlinguette, *Science*, 2013, **340**, 60.
105 S. Zhao, Y. Wang, J. Dong, C.-T. He, H. Yin, P. An, K. Zhao, X. Zhang, C. Gao, L. Zhang, J. Lv, J. Wang, J. Zhang, A. M. Khattak, N. A. Khan, Z. Wei, J. Zhang, S. Liu, H. Zhao and Z. Tang, *Nat. Energy*, 2016, **1**, 16184.
106 L. Zhao, B. Dong, S. Li, L. Zhou, L. Lai, Z. Wang, S. Zhao, M. Han, K. Gao, M. Lu, X. Xie, B. Chen, Z. Liu, X. Wang, H. Zhang, H. Li, J. Liu, H. Zhang, X. Huang and W. Huang, *ACS Nano*, 2017, **11**, 5800.
107 Y. Cao, Z. Zhu, J. Xu, L. Wang, J. Sun, X. Chen and Y. Fan, *Dalton Trans.*, 2015, **44**, 1942.
108 L. Ning, S. Liao, X. Liu, L. Yu, X. Zhuang and X. Tong, *J. Catal.*, 2017, **352**, 480.
109 L. Huang, X. Zhang, Y. Han, Q. Wang, Y. Fang and S. Dong, *J. Mater. Chem. A*, 2017, **5**, 18610.
110 B. Wu, X. Lin, L. Ge, L. Wu and T. Xu, *Chem. Commun.*, 2013, **49**, 143.
111 E. Barankova, X. Tan, L. F. Villalobos, E. Litwiller and K. V. Peinemann, *Angew. Chem., Int. Ed.*, 2017, **56**, 2965.
112 Y. Liu, Y. Ban and W. Yang, *Adv. Mater.*, 2017, **29**, 1606949.
113 S. Qiu, M. Xue and G. Zhu, *Chem. Soc. Rev.*, 2014, **43**, 6116.
114 B. Seoane, J. Coronas, I. Gascon, M. E. Benavides, O. Karvan, J. Caro, F. Kapteijn and J. Gascon, *Chem. Soc. Rev.*, 2015, **44**, 2421.
115 J. Yao and H. Wang, *Chem. Soc. Rev.*, 2014, **43**, 4470.
116 C. Zhang and W. J. Koros, *J. Phys. Chem. Lett.*, 2015, **6**, 3841.
117 W. Li, *Prog. Mater. Sci.*, 2019, **100**, 21.
118 S. Qiu and G. Zhu, *Coord. Chem. Rev.*, 2009, **253**, 2891.
119 A. Knebel, L. Sundermann, A. Mohmeyer, I. Strauß, S. Friebe, P. Behrens and J. r. Caro, *Chem. Mater.*, 2017, **29**, 3111.
120 W. Li, Y. Zhang, Q. Li and G. Zhang, *Chem. Eng. Sci.*, 2015, **135**, 232.
121 W.-J. Li, M. Tu, R. Cao and R. A. Fischer, *J. Mater. Chem. A*, 2016, **4**, 12356.
122 L. Heinke, *J. Phys. D: Appl. Phys.*, 2017, **50**, 193004.
123 A. Bétard, H. Bux, S. Henke, D. Zacher, J. Caro and R. A. Fischer, *Microporous Mesoporous Mater.*, 2012, **150**, 76.
124 S. Horike, S. Shimomura and S. Kitagawa, *Nat. Chem.*, 2009, **1**, 695.
125 C. Ze, Y. Dong-Hui, X. Jian, H. Tong-Liang and B. Xian-He, *Adv. Mater.*, 2015, **27**, 5432.
126 N. C. Burtch, J. Heinen, T. D. Bennett, D. Dubbeldam and M. D. Allendorf, *Adv. Mater.*, 2017, 1704124.
127 Y.-n. Wu, F. Li, H. Liu, W. Zhu, M. Teng, Y. Jiang, W. Li, D. Xu, D. He, P. Hannam and G. Li, *J. Mater. Chem.*, 2012, **22**, 16971.
128 Y. Yoo, V. Varela-Guerrero and H. K. Jeong, *Langmuir*, 2011, **27**, 2652.
129 Y. Yoo and H.-K. Jeong, *Cryst. Growth Des.*, 2010, **10**, 1283.
130 J. Campbell, R. P. Davies, D. C. Braddock and A. G. Livingston, *J. Mater. Chem. A*, 2015, **3**, 9668.
131 F. Cacho-Bailo, S. Catalán-Aguirre, M. Etxeberría-Benavides, O. Karvan, V. Sebastian, C. Téllez and J. Coronas, *J. Membr. Sci.*, 2015, **476**, 277.

132 Z.-G. Gu, A. Pfriem, S. Hamsch, H. Breitwieser, J. Wohlgemuth, L. Heinke, H. Gliemann and C. Wöll, *Microporous Mesoporous Mater.*, 2015, **211**, 82.
133 L. Ge, W. Zhou, V. Rudolph and Z. Zhu, *J. Mater. Chem. A*, 2013, **1**, 6350.
134 M. C. McCarthy, V. Varela-Guerrero, G. V. Barnett and H.-K. Jeong, *Langmuir*, 2010, **26**, 14636.
135 J. Cravillon, C. A. Schröder, H. Bux, A. Rothkirch, J. Caro and M. Wiebcke, *CrystEngComm*, 2012, **14**, 492.
136 M. Shah, H. T. Kwon, V. Tran, S. Sachdeva and H.-K. Jeong, *Microporous Mesoporous Mater.*, 2013, **165**, 63.
137 M. W. Anjum, F. Vermoortele, A. L. Khan, B. Bueken, D. E. De Vos and I. F. Vankelecom, *ACS Appl. Mater. Interfaces*, 2015, **7**, 25193.
138 S. Hermans, E. Dom, H. Mariën, G. Koeckelberghs and I. F. J. Vankelecom, *J. Membr. Sci.*, 2015, **476**, 356.
139 K. Vanherck, G. Koeckelberghs and I. F. J. Vankelecom, *Prog. Polym. Sci.*, 2013, **38**, 874.
140 H. T. Kwon and H. K. Jeong, *J. Am. Chem. Soc.*, 2013, **135**, 10763.
141 E. Shamsaei, X. Lin, Z. X. Low, Z. Abbasi, Y. Hu, J. Z. Liu and H. Wang, *ACS Appl. Mater. Interfaces*, 2016, **8**, 6236.
142 J. Yao, D. Dong, D. Li, L. He, G. Xu and H. Wang, *Chem. Commun.*, 2011, **47**, 2559.
143 Z. Kang, L. Fan and D. Sun, *J. Mater. Chem. A*, 2017, **5**, 10073.
144 B. P. Biswal, A. Bhaskar, R. Banerjee and U. K. Kharul, *Nanoscale*, 2015, **7**, 7291.
145 M. N. Shah, M. A. Gonzalez, M. C. McCarthy and H. K. Jeong, *Langmuir*, 2013, **29**, 7896.
146 J. Zhu, L. Qin, A. Uliana, J. Hou, J. Wang, Y. Zhang, X. Li, S. Yuan, J. Li, M. Tian, J. Lin and B. Van der Bruggen, *ACS Appl. Mater. Interfaces*, 2017, **9**, 1975.
147 C. Echaide-Gorriz, M. Navarro, C. Tellez and J. Coronas, *Dalton Trans.*, 2017, **46**, 6244.
148 G. Wu, J. Huang, Y. Zang, J. He and G. Xu, *J. Am. Chem. Soc.*, 2017, **139**, 1360.
149 Y. Zhang, X. Feng, H. Li, Y. Chen, J. Zhao, S. Wang, L. Wang and B. Wang, *Angew. Chem., Int. Ed.*, 2015, **54**, 4259.
150 Y. Mao, J. Li, W. Cao, Y. Ying, L. Sun and X. Peng, *ACS Appl. Mater. Interfaces*, 2014, **6**, 4473.
151 S. Hurrle, S. Friebe, J. Wohlgemuth, C. Wçll, J. Caro and L. Heinke, *Chem.–Eur. J.*, 2017, **23**, 2294.
152 X. Ma, P. Kumar, N. Mittal, A. Khlyustova, P. Daoutidis, K. A. Mkhoyan and M. Tsapatsis, *Science*, 2018, **361**, 1008.
153 P. Marchetti, M. F. Jimenez Solomon, G. Szekely and A. G. Livingston, *Chem. Rev.*, 2014, **114**, 10735.
154 B. Liang, H. Wang, X. Shi, B. Shen, X. He, Z. A. Ghazi, N. A. Khan, H. Sin, A. M. Khattak, L. Li and Z. Tang, *Nat. Chem.*, 2018, **10**, 961.
155 S. Keskin and D. S. Sholl, *J. Phys. Chem. C*, 2007, **111**, 14055.
156 T. C. Merkel, B. D. Freeman, R. J. Spontak, Z. He, I. Pinnau, P. Meakin and A. J. Hill, *Science*, 2002, **296**, 519.
157 P. Kamakoti, B. D. Morreale, M. V. Ciocco, B. H. Howard, R. P. Killmeyer, A. V. Cugini and D. S. Sholl, *Science*, 2005, **307**, 569.
158 J. R. Li, R. J. Kuppler and H. C. Zhou, *Chem. Soc. Rev.*, 2009, **38**, 1477.
159 A. M. Mosier, H. L. Larson, E. R. Webster, M. Ivos, F. Tian and L. Benz, *Langmuir*, 2016, **32**, 2947.
160 M. S. Denny Jr, J. C. Moreton, L. Benz and S. M. Cohen, *Nat. Rev. Mater.*, 2016, **1**, 16078.
161 X.-L. Liu, Y.-S. Li, G.-Q. Zhu, Y.-J. Ban, L.-Y. Xu and W.-S. Yang, *Angew. Chem., Int. Ed.*, 2011, **50**, 10636.
162 Y. Li and W. Yang, *Chin. J. Catal.*, 2015, **36**, 692.
163 H. L. Jiang and Q. Xu, *Chem. Commun.*, 2011, **47**, 3351.
164 B. Seoane, S. Castellanos, A. Dikhtiarenko, F. Kapteijn and J. Gascon, *Coord. Chem. Rev.*, 2016, **307**, 147.
165 S. R. Venna and M. A. Carreon, *Chem. Eng. Sci.*, 2015, **124**, 3.
166 E. Ilknur, Y. Gamze and K. Seda, *Chem.–Asian J.*, 2013, **8**, 1692.
167 J. Gascon, F. Kapteijn, B. Zornoza, V. Sebastián, C. Casado and J. Coronas, *Chem. Mater.*, 2012, **24**, 2829.
168 E. Adatoz, A. K. Avci and S. Keskin, *Sep. Purif. Technol.*, 2015, **152**, 207.
169 Z. Zhang, Z.-Z. Yao, S. Xiang and B. Chen, *Energy Environ. Sci.*, 2014, **7**, 2868.
170 X. Li, Y. Liu, J. Wang, J. Gascon, J. Li and B. Van der Bruggen, *Chem. Soc. Rev.*, 2017, **46**, 7124.
171 H. Li, K. Wang, Y. Sun, C. T. Lollar, J. Li and H.-C. Zhou, *Mater. Today*, 2018, **21**, 108.
172 M. Vinoba, M. Bhagiyalakshmi, Y. Alqaheem, A. A. Alomair, A. Pérez and M. S. Rana, *Sep. Purif. Technol.*, 2017, **188**, 431.
173 J. Hou, P. D. Sutrisna, Y. Zhang and V. Chen, *Angew. Chem., Int. Ed.*, 2016, **55**, 3947.
174 Y. Peng, Y. Li, Y. Ban, H. Jin, W. Jiao, X. Liu and W. Yang, *Science*, 2014, **346**, 1356.
175 S. Shahid and K. Nijmeijer, *J. Membr. Sci.*, 2014, **470**, 166.
176 Y. Zhu, J. Ciston, B. Zheng, X. Miao, C. Czarnik, Y. Pan, R. Sougrat, Z. Lai, C. E. Hsiung, K. Yao, I. Pinnau, M. Pan and Y. Han, *Nat. Mater.*, 2017, **16**, 532.
177 X. Liu, H. Jin, Y. Li, H. Bux, Z. Hu, Y. Ban and W. Yang, *J. Membr. Sci.*, 2013, **428**, 498.
178 L. Kong, G. Zhang, H. Liu and X. Zhang, *Mater. Lett.*, 2015, **141**, 344.
179 S.-L. Li and Q. Xu, *Energy Environ. Sci.*, 2013, **6**, 1656.
180 X. Gao, X. Zou, H. Ma, S. Meng and G. Zhu, *Adv. Mater.*, 2014, **26**, 3644.
181 S. Yu, F. Pan, S. Yang, H. Ding, Z. Jiang, B. Wang, Z. Li and X. Cao, *Chem. Eng. Sci.*, 2015, **135**, 479.
182 N. C. Su, D. T. Sun, C. M. Beavers, D. K. Britt, W. L. Queen and J. J. Urban, *Energy Environ. Sci.*, 2016, **9**, 922.
183 N. Rangnekar, N. Mittal, B. Elyassi, J. Caro and M. Tsapatsis, *Chem. Soc. Rev.*, 2015, **44**, 7128.
184 J. Sun, A. Klechikov, C. Moise, M. Prodana, M. Enachescu and A. V. Talyzin, *Angew. Chem., Int. Ed.*, 2018, **57**, 1034.
185 A. P. Côté, A. I. Benin, N. W. Ockwig, M. O'Keeffe, A. J. Matzger and O. M. Yaghi, *Science*, 2005, **310**, 1166.
186 N. Huang, P. Wang and D. Jiang, *Nat. Rev. Mater.*, 2016, **1**, 16068.
187 S. Kandambeth, V. Venkatesh, D. B. Shinde, S. Kumari, A. Halder, S. Verma and R. Banerjee, *Nat. Commun.*, 2015, **6**, 6786.

188 N. A. H. Md Nordin, S. M. Racha, T. Matsuura, N. Misdan, N. A. Abdullah Sani, A. F. Ismail and A. Mustafa, *RSC Adv.*, 2015, **5**, 43110.
189 B. Zornoza, A. Martinez-Joaristi, P. Serra-Crespo, C. Tellez, J. Coronas, J. Gascon and F. Kapteijn, *Chem. Commun.*, 2011, **47**, 9522.
190 S. Sorribas, P. Gorgojo, C. Tellez, J. Coronas and A. G. Livingston, *J. Am. Chem. Soc.*, 2013, **135**, 15201.
191 F. Cacho-Bailo, C. Tellez and J. Coronas, *Chemistry*, 2016, **22**, 9533.
192 A. Kertik, L. H. Wee, M. Pfannmöller, S. Bals, J. A. Martens and I. F. J. Vankelecom, *Energy Environ. Sci.*, 2017, **10**, 2342.
193 H.-L. Jiang, Q.-P. Lin, T. Akita, B. Liu, H. Ohashi, H. Oji, T. Honma, T. Takei, M. Haruta and Q. Xu, *Chem.–Asian J.*, 2011, **17**, 78.
194 L. Hou, W.-J. Shi, Y.-Y. Wang, Y. Guo, C. Jin and Q.-Z. Shi, *Chem. Commun.*, 2011, **47**, 5464.
195 R. Lin, L. Ge, L. Hou, E. Strounina, V. Rudolph and Z. Zhu, *ACS Appl. Mater. Interfaces*, 2014, **6**, 5609.
196 D. Nagaraju, D. G. Bhagat, R. Banerjee and U. K. Kharul, *J. Mater. Chem. A*, 2013, **1**, 8828.
197 H. B. Tanh Jeazet, S. Sorribas, J. M. Román-Marín, B. Zornoza, C. Téllez, J. Coronas and C. Janiak, *Eur. J. Inorg. Chem.*, 2016, **2016**, 4363.
198 L. Lin, L. Zhang, C. Zhang, M. Dong, C. Liu, A. Wang, Y. Chu, Y. Zhang and Z. Cao, *RSC Adv.*, 2013, **3**, 9889.
199 M. R. Khdhayyer, E. Esposito, A. Fuoco, M. Monteleone, L. Giorno, J. C. Jansen, M. P. Attfield and P. M. Budd, *Sep. Purif. Technol.*, 2017, **173**, 304.
200 J. Ploegmakers, S. Japip and K. Nijmeijer, *J. Membr. Sci.*, 2013, **428**, 331.
201 S. Y. Lim, J. Choi, H.-Y. Kim, Y. Kim, S.-J. Kim, Y. S. Kang and J. Won, *J. Membr. Sci.*, 2014, **467**, 67.
202 J. Kim, J. Choi, Y. Soo Kang and J. Won, *J. Appl. Polym. Sci.*, 2016, **133**, 42853.
203 K. Xie, Q. Fu, C. Xu, H. Lu, Q. Zhao, R. Curtain, D. Gu, P. A. Webley and G. G. Qiao, *Energy Environ. Sci.*, 2018, **11**, 544.
204 R. Lin, L. Ge, H. Diao, V. Rudolph and Z. Zhu, *ACS Appl. Mater. Interfaces*, 2016, **8**, 32041.
205 Y. Chen, Z. Hu, K. M. Gupta and J. Jiang, *J. Phys. Chem. C*, 2011, **115**, 21736.
206 K. M. Gupta, Y. Chen, Z. Hu and J. Jiang, *Phys. Chem. Chem. Phys.*, 2012, **14**, 5785.
207 K. Fujie and H. Kitagawa, *Coord. Chem. Rev.*, 2016, **307**, 382.
208 E. Adatoz and S. Keskin, *J. Nanomater.*, 2015, **2015**, 1.
209 Z. Sumer and S. Keskin, *Ind. Eng. Chem. Res.*, 2017, **56**, 8713.
210 D. X. Trinh, T. P. N. Tran and T. Taniike, *Sep. Purif. Technol.*, 2017, **177**, 249.
211 Z. Chang, D. H. Yang, J. Xu, T. L. Hu and X. H. Bu, *Adv. Mater.*, 2015, **27**, 5432.
212 A. Knebel, B. Geppert, K. Volgmann, D. I. Kolokolov, A. G. Stepanov, J. Twiefel, P. Heitjans, D. Volkmer and J. Caro, *Science*, 2017, **358**, 347.
213 N. Hara, M. Yoshimune, H. Negishi, K. Haraya, S. Hara and T. Yamaguchi, *RSC Adv.*, 2013, **3**, 14233.
214 Z. Qiao, C. Peng, J. Zhou and J. Jiang, *J. Mater. Chem. A*, 2016, **4**, 15904.
215 K. Otsubo and H. Kitagawa, *APL Mater.*, 2014, **2**, 124105.
216 Y. Mao, B. Su, W. Cao, J. Li, Y. Ying, W. Ying, Y. Hou, L. Sun and X. Peng, *ACS Appl. Mater. Interfaces*, 2014, **6**, 15676.
217 Z. Wang, P. G. Weidler, C. Azucena, L. Heinke and C. Wöll, *Microporous Mesoporous Mater.*, 2016, **222**, 241.
218 Y. V. Kaneti, S. Dutta, M. S. A. Hossain, M. J. A. Shiddiky, K. L. Tung, F. K. Shieh, C. K. Tsung, K. C. Wu and Y. Yamauchi, *Adv. Mater.*, 2017, **29**, 1700213.
219 H. B. Tanh Jeazet, C. Staudt and C. Janiak, *Dalton Trans.*, 2012, **41**, 14003.
220 N. Stock and S. Biswas, *Chem. Rev.*, 2012, **112**, 933.
221 C. Kong, H. Du, L. Chen and B. Chen, *Energy Environ. Sci.*, 2017, **10**, 1812.
222 X. Qin, Y. Sun, N. Wang, Q. Wei, L. Xie, Y. Xie and J.-R. Li, *RSC Adv.*, 2016, **6**, 94177.
223 Y. Jiang, G. H. Ryu, S. H. Joo, X. Chen, S. H. Lee, X. Chen, M. Huang, X. Wu, D. Luo, Y. Huang, J. H. Lee, B. Wang, X. Zhang, S. K. Kwak, Z. Lee and R. S. Ruoff, *ACS Appl. Mater. Interfaces*, 2017, **9**, 28107.
224 S. Basu, A. Cano-Odena and I. F. J. Vankelecom, *Sep. Purif. Technol.*, 2011, **81**, 31.
225 M. Matsumoto and T. Kitaoka, *Adv. Mater.*, 2016, **28**, 1765.
226 R. Lin, L. Ge, S. Liu, V. Rudolph and Z. Zhu, *ACS Appl. Mater. Interfaces*, 2015, **7**, 14750.
227 S. Keskin and D. S. Sholl, *Energy Environ. Sci.*, 2010, **3**, 343.
228 Z. Feng, Z. Xiaoqin, G. Xue, F. Songjie, S. Fuxing, R. Hao and Z. Guangshan, *Adv. Funct. Mater.*, 2012, **22**, 3583.
229 F. Cacho-Bailo, G. Caro, M. Etxeberría-Benavides, O. Karvan, C. Téllez and J. Coronas, *RSC Adv.*, 2016, **6**, 5881.
230 T. Rodenas, I. Luz, G. Prieto, B. Seoane, H. Miro, A. Corma, F. Kapteijn, I. X. F. X. Llabres and J. Gascon, *Nat. Mater.*, 2015, **14**, 48.
231 X. Dong, K. Huang, S. Liu, R. Ren, W. Jin and Y. S. Lin, *J. Mater. Chem.*, 2012, **22**, 19222.
232 J. Ploegmakers, S. Japip and K. Nijmeijer, *J. Membr. Sci.*, 2013, **428**, 445.
233 S. R. Venna and M. A. Carreon, *J. Am. Chem. Soc.*, 2010, **132**, 76.
234 Y. Liu, G. Zeng, Y. Pan and Z. Lai, *J. Membr. Sci.*, 2011, **379**, 46.
235 Y. Li, F. Liang, H. Bux, W. Yang and J. Caro, *J. Membr. Sci.*, 2010, **354**, 48.
236 D. Ragab, H. G. Gomaa, R. Sabouni, M. Salem, M. Ren and J. Zhu, *Chem. Eng. J.*, 2016, **300**, 273.
237 Z. Shi, C. Xu, F. Chen, Y. Wang, L. Li, Q. Meng and R. Zhang, *RSC Adv.*, 2017, **7**, 49947.
238 M. Ding, W. Shi, L. Guo, Z. Y. Leong, A. Baji and H. Y. Yang, *J. Mater. Chem. A*, 2017, **5**, 6113.
239 P. Ramaswamy, N. E. Wong and G. K. Shimizu, *Chem. Soc. Rev.*, 2014, **43**, 5913.
240 J. Zhou and B. Wang, *Chem. Soc. Rev.*, 2017, **46**, 6927.
241 K. Fu, Y. Gong, G. T. Hitz, D. W. McOwen, Y. Li, S. Xu, Y. Wen, L. Zhang, C. Wang, G. Pastel, J. Dai, B. Liu, H. Xie, Y. Yao, E. D. Wachsman and L. Hu, *Energy Environ. Sci.*, 2017, **10**, 1568.

242 J. van den Broek, S. Afyon and J. L. M. Rupp, *Adv. Energy Mater.*, 2016, **6**, 1600736.
243 Z. Wang, R. Tan, H. Wang, L. Yang, J. Hu, H. Chen and F. Pan, *Adv. Mater.*, 2018, **30**, 1704436.
244 J.-K. Sun and Q. Xu, *Energy Environ. Sci.*, 2014, **7**, 2071.
245 F.-F. Cao, Y.-G. Guo and L.-J. Wan, *Energy Environ. Sci.*, 2011, **4**, 1634.
246 P. G. Bruce, B. Scrosati and J.-M. Tarascon, *Angew. Chem., Int. Ed.*, 2008, **47**, 2930.
247 M. V. Reddy, G. V. Subba Rao and B. V. R. Chowdari, *Chem. Rev.*, 2013, **113**, 5364.
248 S. Xin, Y.-G. Guo and L.-J. Wan, *Acc. Chem. Res.*, 2012, **45**, 1759.
249 C. Liu, F. Li, L.-P. Ma and H.-M. Cheng, *Adv. Mater.*, 2010, **22**, E28.
250 S. Liu, Z. Wang, C. Yu, H. B. Wu, G. Wang, Q. Dong, J. Qiu, A. Eychmüller and X. W. Lou, *Adv. Mater.*, 2013, **25**, 3462.
251 B. Y. Guan, X. Y. Yu, H. B. Wu and X. W. D. Lou, *Adv. Mater.*, 2017, **29**, 1703614.
252 R. Wu, X. Qian, X. Rui, H. Liu, B. Yadian, K. Zhou, J. Wei, Q. Yan, X. Q. Feng, Y. Long, L. Wang and Y. Huang, *Small*, 2014, **10**, 1932.
253 F. Zheng, D. Zhu, X. Shi and Q. Chen, *J. Mater. Chem. A*, 2015, **3**, 2815.
254 X. Ge, Z. Li, C. Wang and L. Yin, *ACS Appl. Mater. Interfaces*, 2015, **7**, 26633.
255 G. Fang, Z. Wu, J. Zhou, C. Zhu, X. Cao, T. Lin, Y. Chen, C. Wang, A. Pan and S. Liang, *Adv. Energy Mater.*, 2018, **8**, 1703155.
256 G. Fang, J. Zhou, Y. Cai, S. Liu, X. Tan, A. Pan and S. Liang, *J. Mater. Chem. A*, 2017, **5**, 13983.
257 S. Liu, J. Zhou, Z. Cai, G. Fang, Y. Cai, A. Pan and S. Liang, *J. Mater. Chem. A*, 2016, **4**, 17838.
258 G. Fang, Q. Wang, J. Zhou, Y. Lei, Z. Chen, Z. Wang, A. Pan and S. Liang, *ACS Nano*, 2019, **13**, 5635.
259 Y. Cai, H. Yang, J. Zhou, Z. Luo, G. Fang, S. Liu, A. Pan and S. Liang, *Chem. Eng. J.*, 2017, **327**, 522.
260 S. Hermes, F. Schröder, R. Chelmowski, C. Wöll and R. A. Fischer, *J. Am. Chem. Soc.*, 2005, **127**, 13744.
261 D. Zacher, O. Shekhah, C. Wöll and R. A. Fischer, *Chem. Soc. Rev.*, 2009, **38**, 1418.
262 P.-C. Guo, T.-Y. Chen, X.-M. Ren, Z. Chu and W. Jin, *J. Mater. Chem. A*, 2014, **2**, 13698.
263 Y. Mao, J. Li, W. Cao, Y. Ying, P. Hu, Y. Liu, L. Sun, H. Wang, C. Jin and X. Peng, *Nat. Commun.*, 2014, **5**, 5532.
264 X. Peng, J. Jin, E. M. Ericsson and I. Ichinose, *J. Am. Chem. Soc.*, 2007, **129**, 8625.
265 J. J. Gassensmith, P. M. Erne, W. F. Paxton, C. Valente and J. F. Stoddart, *Langmuir*, 2011, **27**, 1341.
266 R. L. Papporello, E. E. Miró and J. M. Zamaro, *Microporous Mesoporous Mater.*, 2015, **211**, 64.
267 M. Li and M. Dincă, *J. Am. Chem. Soc.*, 2011, **133**, 12926.
268 H. Al-Kutubi, J. Gascon, E. J. R. Sudhölter and L. Rassaei, *ChemElectroChem*, 2015, **2**, 462.
269 R. Kaur, K.-H. Kim and A. Deep, *Appl. Surf. Sci.*, 2017, **396**, 1303.
270 H. Liu, H. Wang, T. Chu, M. Yu and Y. Yang, *J. Mater. Chem. C*, 2014, **2**, 8683.
271 W. J. Li, J. F. Feng, Z. J. Lin, Y. L. Yang, Y. Yang, X. S. Wang, S. Y. Gao and R. Cao, *Chem. Commun.*, 2016, **52**, 3951.
272 D. Bradshaw, A. Garai and J. Huo, *Chem. Soc. Rev.*, 2012, **41**, 2344.
273 M. Zhou, J. Li, M. Zhang, H. Wang, Y. Lan, Y. N. Wu, F. Li and G. Li, *Chem. Commun.*, 2015, **51**, 2706.
274 K. Otsubo, T. Haraguchi, O. Sakata, A. Fujiwara and H. Kitagawa, *J. Am. Chem. Soc.*, 2012, **134**, 9605.
275 S. Osama, W. Hui, Z. Denise, A. F. Roland and W. Christof, *Angew. Chem., Int. Ed.*, 2009, **48**, 5038.
276 V. Stavila, C. Schneider, C. Mowry, T. R. Zeitler, J. A. Greathouse, A. L. Robinson, J. M. Denning, J. Volponi, K. Leong, W. Quan, M. Tu, R. A. Fischer and M. D. Allendorf, *Adv. Funct. Mater.*, 2016, **26**, 1699.
277 T. Haraguchi, K. Otsubo, O. Sakata, A. Fujiwara and H. Kitagawa, *Inorg. Chem.*, 2015, **54**, 11593.
278 R. Makiura, S. Motoyama, Y. Umemura, H. Yamanaka, O. Sakata and H. Kitagawa, *Nat. Mater.*, 2010, **9**, 565.
279 O. Shekhah, *Materials*, 2010, **3**, 1302.
280 Y. Chen, S. Li, X. Pei, J. Zhou, X. Feng, S. Zhang, Y. Cheng, H. Li, R. Han and B. Wang, *Angew. Chem., Int. Ed.*, 2016, **55**, 3419.
281 H. Gliemann and C. Wöll, *Mater. Today*, 2012, **15**, 110.
282 Z. Wang, J. Liu, H. K. Arslan, S. Grosjean, T. Hagendorn, H. Gliemann, S. Bräse and C. Wöll, *Langmuir*, 2013, **29**, 15958.
283 M. S. Yao, X. J. Lv, Z. H. Fu, W. H. Li, W. H. Deng, G. D. Wu and G. Xu, *Angew. Chem., Int. Ed.*, 2017, **56**, 16510.
284 W.-Q. Fu, M. Liu, Z.-G. Gu, S.-M. Chen and J. Zhang, *Cryst. Growth Des.*, 2016, **16**, 5487.
285 Z. G. Gu, Z. Chen, W. Q. Fu, F. Wang and J. Zhang, *ACS Appl. Mater. Interfaces*, 2015, **7**, 28585.
286 V. Chernikova, O. Shekhah, I. Spanopoulos, P. N. Trikalitis and M. Eddaoudi, *Chem. Commun.*, 2017, **53**, 6191.
287 S. Wannapaiboon, M. Tu and R. A. Fischer, *Adv. Funct. Mater.*, 2014, **24**, 2696.
288 S. Wannapaiboon, M. Tu, K. Sumida, K. Khaletskaya, S. Furukawa, S. Kitagawa and R. A. Fischer, *J. Mater. Chem. A*, 2015, **3**, 23385.
289 M. Meilikhov, S. Furukawa, K. Hirai, R. A. Fischer and S. Kitagawa, *Angew. Chem., Int. Ed.*, 2013, **52**, 341.
290 O. Shekhah, H. Wang, S. Kowarik, F. Schreiber, M. Paulus, M. Tolan, C. Sternemann, F. Evers, D. Zacher, R. A. Fischer and C. Wöll, *J. Am. Chem. Soc.*, 2007, **129**, 15118.
291 J.-L. Zhuang, A. Terfort and C. Wöll, *Coord. Chem. Rev.*, 2016, **307**, 391.
292 E. Redel, Z. Wang, S. Walheim, J. Liu, H. Gliemann and C. Wöll, *Appl. Phys. Lett.*, 2013, **103**, 091903.
293 C. Hermosa, B. R. Horrocks, J. I. Martinez, F. Liscio, J. Gomez-Herrero and F. Zamora, *Chem. Sci.*, 2015, **6**, 2553.
294 V. Chernikova, O. Shekhah and M. Eddaoudi, *ACS Appl. Mater. Interfaces*, 2016, **8**, 20459.
295 P. Burmann, B. Zornoza, C. Téllez and J. Coronas, *Chem. Eng. Sci.*, 2014, **107**, 66.

296 Q. Song, S. Jiang, T. Hasell, M. Liu, S. Sun, A. K. Cheetham, E. Sivaniah and A. I. Cooper, *Adv. Mater.*, 2016, **28**, 2629.
297 K. B. Lausund and O. Nilsen, *Nat. Commun.*, 2016, **7**, 13578.
298 K. B. Klepper, O. Nilsen and H. Fjellvag, *Dalton Trans.*, 2010, **39**, 11628.
299 J. H. Cavka, S. Jakobsen, U. Olsbye, N. Guillou, C. Lamberti, S. Bordiga and K. P. Lillerud, *J. Am. Chem. Soc.*, 2008, **130**, 13850.
300 K. Khaletskaya, S. Turner, M. Tu, S. Wannapaiboon, A. Schneemann, R. Meyer, A. Ludwig, G. Van Tendeloo and R. A. Fischer, *Adv. Funct. Mater.*, 2014, **24**, 4804.
301 Y. Wang, M. Zhao, J. Ping, B. Chen, X. Cao, Y. Huang, C. Tan, Q. Ma, S. Wu, Y. Yu, Q. Lu, J. Chen, W. Zhao, Y. Ying and H. Zhang, *Adv. Mater.*, 2016, **28**, 4149.
302 Y. Abdollahian, J. L. Hauser, I. R. Colinas, C. Agustin, A. S. Ichimura and S. R. J. Oliver, *Cryst. Growth Des.*, 2014, **14**, 1506.
303 D. Feng, Z.-Y. Gu, J.-R. Li, H.-L. Jiang, Z. Wei and H.-C. Zhou, *Angew. Chem., Int. Ed.*, 2012, **51**, 10307.
304 W. Morris, B. Volosskiy, S. Demir, F. Gándara, P. L. McGrier, H. Furukawa, D. Cascio, J. F. Stoddart and O. M. Yaghi, *Inorg. Chem.*, 2012, **51**, 6443.
305 S. M. Yoon, J. H. Park and B. A. Grzybowski, *Angew. Chem., Int. Ed.*, 2017, **56**, 127.
306 I. Stassen, M. Styles, G. Grenci, H. V. Gorp, W. Vanderlinden, S. D. Feyter, P. Falcaro, D. D. Vos, P. Vereecken and R. Ameloot, *Nat. Mater.*, 2015, **15**, 304.
307 D. Fischer, A. von Mankowski, A. Ranft, S. K. Vasa, R. Linser, J. Mannhart and B. V. Lotsch, *Chem. Mater.*, 2017, **29**, 5148.
308 M. D. Allendorf, C. A. Bauer, R. K. Bhakta and R. J. Houk, *Chem. Soc. Rev.*, 2009, **38**, 1330.
309 W. P. Lustig, S. Mukherjee, N. D. Rudd, A. V. Desai, J. Li and S. K. Ghosh, *Chem. Soc. Rev.*, 2017, **46**, 3242.
310 P. R. Matthes and K. Müller-Buschbaum, *Z. Anorg. Allg. Chem.*, 2014, **640**, 2847.
311 L. V. Meyer, F. Schonfeld and K. Muller-Buschbaum, *Chem. Commun.*, 2014, **50**, 8093.
312 J. Troyano, Ó. Castillo, P. Amo-Ochoa, V. Fernández-Moreira, C. J. Gómez-García, F. Zamora and S. Delgado, *J. Mater. Chem. C*, 2016, **4**, 8545.
313 J. Conesa-Egea, N. Nogal, J. I. Martínez, V. Fernández-Moreira, U. R. Rodríguez-Mendoza, J. González-Platas, C. J. Gómez-García, S. Delgado, F. Zamora and P. Amo-Ochoa, *Chem. Sci.*, 2018, **9**, 8000.
314 N. Campagnol, E. R. Souza, D. E. De Vos, K. Binnemans and J. Fransaer, *Chem. Commun.*, 2014, **50**, 12545.
315 L. V. Meyer, J. Vogt, F. A. Brede, H. Schäfer, M. Steinhart and K. Müller-Buschbaum, *CrystEngComm*, 2013, **15**, 9382.
316 S. Parshamoni, J. Telangae and S. Konar, *Dalton Trans.*, 2015, **44**, 20926.
317 L. E. Kreno, J. T. Hupp and R. P. V. Duyne, *Anal. Chem.*, 2010, **82**, 8042.
318 A. H. Assen, O. Yassine, O. Shekhah, M. Eddaoudi and K. N. Salama, *ACS Sens.*, 2017, **2**, 1294.
319 Z. Dou, J. Yu, Y. Cui, Y. Yang, Z. Wang, D. Yang and G. Qian, *J. Am. Chem. Soc.*, 2014, **136**, 5527.
320 O. Yassine, O. Shekhah, A. H. Assen, Y. Belmabkhout, K. N. Salama and M. Eddaoudi, *Angew. Chem., Int. Ed.*, 2016, **55**, 15879.
321 R. Elzein, C. M. Chang, I. Ponomareva, W. Y. Gao, S. Ma and R. Schlaf, *ACS Appl. Mater. Interfaces*, 2016, **8**, 31403.
322 A. A. Talin, A. Centrone, A. C. Ford, M. E. Foster, V. Stavila, P. Haney, R. A. Kinney, V. Szalai, F. E. Gabaly, H. P. Yoon, F. Léonard and M. D. Allendorf, *Science*, 2014, **343**, 66.
323 Z. Guo, D. K. Panda, K. Maity, D. Lindsey, T. G. Parker, T. E. Albrecht-Schmitt, J. L. Barreda-Esparza, P. Xiong, W. Zhou and S. Saha, *J. Mater. Chem. C*, 2016, **4**, 894.
324 Y. Liu, H. Wang, W. Shi, W. Zhang, J. Yu, B. K. Chandran, C. Cui, B. Zhu, Z. Liu, B. Li, C. Xu, Z. Xu, S. Li, W. Huang, F. Huo and X. Chen, *Angew. Chem., Int. Ed.*, 2016, **55**, 8884.
325 M.-J. Park and J.-S. Lee, *RSC Adv.*, 2017, **7**, 21045.
326 J. W. Maina, J. A. Schutz, L. Grundy, E. Des Ligneris, Z. Yi, L. Kong, C. Pozo-Gonzalo, M. Ionescu and L. F. Dumee, *ACS Appl. Mater. Interfaces*, 2017, **9**, 35010.
327 P. Wu, X. Guo, L. Cheng, C. He, J. Wang and C. Duan, *Inorg. Chem.*, 2016, **55**, 8153.
328 N. Kornienko, Y. Zhao, C. S. Kley, C. Zhu, D. Kim, S. Lin, C. J. Chang, O. M. Yaghi and P. Yang, *J. Am. Chem. Soc.*, 2015, **137**, 14129.
329 H. Furukawa, N. Ko, Y. B. Go, N. Aratani, S. B. Choi, E. Choi, A. Ö. Yazaydin, R. Q. Snurr, M. O'Keeffe, J. Kim and O. M. Yaghi, *Science*, 2010, **329**, 424.
330 X. Shen and B. Yan, *Dalton Trans.*, 2015, **44**, 1875.
331 M. Tsotsalas, J. Liu, B. Tettmann, S. Grosjean, A. Shahnas, Z. Wang, C. Azucena, M. Addicoat, T. Heine, J. Lahann, J. Overhage, S. Bräse, H. Gliemann and C. Wöll, *J. Am. Chem. Soc.*, 2014, **136**, 8.
332 J. X. Wu and B. Yan, *Dalton Trans.*, 2016, **45**, 18585.
333 D. Wisser, F. M. Wisser, S. Raschke, N. Klein, M. Leistner, J. Grothe, E. Brunner and S. Kaskel, *Angew. Chem., Int. Ed.*, 2015, **54**, 12588.
334 D. Liu, J. Gu, Q. Liu, Y. Tan, Z. Li, W. Zhang, Y. Su, W. Li, A. Cui, C. Gu and D. Zhang, *Adv. Mater.*, 2014, **26**, 1229.
335 I. Stassen, N. Campagnol, J. Fransaer, P. Vereecken, D. De Vos and R. Ameloot, *CrystEngComm*, 2013, **15**, 9308.
336 D. Liu, D. Zou, H. Zhu and J. Zhang, *Small*, 2018, **14**, 1801454.
337 M. Zhao, K. Yuan, Y. Wang, G. Li, J. Guo, L. Gu, W. Hu, H. Zhao and Z. Tang, *Nature*, 2016, **539**, 76.
338 Y. Gu, Y. N. Wu, L. Li, W. Chen, F. Li and S. Kitagawa, *Angew. Chem., Int. Ed.*, 2017, **56**, 15658.
339 Y. Peng, M. Zhao, B. Chen, Z. Zhang, Y. Huang, F. Dai, Z. Lai, X. Cui, C. Tan and H. Zhang, *Adv. Mater.*, 2018, **30**, 1705454.
340 L. R. Parent, C. H. Pham, J. P. Patterson, M. S. Denny Jr, S. M. Cohen, N. C. Gianneschi and F. Paesani, *J. Am. Chem. Soc.*, 2017, **139**, 13973.
341 K. M. Choi, H. M. Jeong, J. H. Park, Y.-B. Zhang, J. K. Kang and O. M. Yaghi, *ACS Nano*, 2014, **8**, 7451.
342 W. Zeng, L. Wang, H. Shi, G. Zhang, K. Zhang, H. Zhang, F. Gong, T. Wang and H. Duan, *J. Mater. Chem. A*, 2016, **4**, 8233.

343 Y. Jiao, J. Pei, D. Chen, C. Yan, Y. Hu, Q. Zhang and G. Chen, *J. Mater. Chem. A*, 2017, **5**, 1094.
344 X. Yan, X. Li, Z. Yan and S. Komarneni, *Appl. Surf. Sci.*, 2014, **308**, 306.
345 S. Chen, M. Xue, Y. Li, Y. Pan, L. Zhu and S. Qiu, *J. Mater. Chem. A*, 2015, **3**, 20145.
346 X. Xu, J. Tang, H. Qian, S. Hou, Y. Bando, M. S. A. Hossain, L. Pan and Y. Yamauchi, *ACS Appl. Mater. Interfaces*, 2017, **9**, 38737.
347 Y. Liu, G. Li, Y. Guo, Y. Ying and X. Peng, *ACS Appl. Mater. Interfaces*, 2017, **9**, 14043.
348 K. Zagorodniy, G. Seifert and H. Hermann, *Appl. Phys. Lett.*, 2010, **97**, 251905.
349 Y. Zhou and B. Yan, *J. Mater. Chem. C*, 2015, **3**, 8413.
350 J. Chen, X. Zhang, C. Huang, H. Cai, S. Hu, Q. Wan, X. Pei and J. Wang, *J. Biomed. Mater. Res., Part A*, 2017, **105**, 834.